

International Association of Sedimentologists

Field Excursion Guidebook

**Carbonates bounding glacial deposits: Evidence for
Snowball Earth episodes and greenhouse aftermaths
in the Neoproterozoic Otavi Group of northern Namibia**

Excursion leader: Paul F. Hoffman, Harvard University

July 1-7, 2002

(Use Fig. 6 for cover.)

CONTENTS

| | |
|--|--------|
| Introduction | page 3 |
| Regional setting | 3 |
| Stratigraphic development | 5 |
| Ombombo subgroup | 5 |
| Chuosi glaciation | 7 |
| Rasthof cap-carbonate sequence | 8 |
| Upper Abenab subgroup | 10 |
| Ghaub glaciation | 11 |
| Maieberg cap-carbonate sequence | 12 |
| Upper Tsumeb subgroup | 13 |
| Mulden Group | 14 |
| Discussion | 14 |
| Daily excursion log | 15 |
| Day 1: Travel Windhoek to upper Huab River | 15 |
| Day 2: Ghaub-bounding carbonates on the Huab ridge | 15 |
| Day 3: Ghaub-bounding carbonates on the Fransfontein slope | 22 |
| Day 4: Travel Fransfontein slope to Hoanib shelf | 25 |
| Day 5: Chuosi-bounding carbonates on the Hoanib shelf | 26 |
| Day 6: Ghaub-bounding carbonates on the Hoanib shelf | 33 |
| Day 7: Return to Windhoek | 35 |
| Acknowledgements | 35 |
| References | 36 |

INTRODUCTION

Nowhere is the Neoproterozoic climatic paradox posed by closely associated glacial diamictite and carbonate (Spencer, 1972; Fairchild, 1995) more blatant than in the Otavi Group of northern Namibia. Of all the many late Neoproterozoic successions bearing glacial deposits (Hambrey and Harland, 1981; Evans, 2000), none is richer in carbonate. This also makes the Otavi Group ideally suited for carbon isotope chemostratigraphy, which revolutionized the study of late Neoproterozoic Earth history in the 1990s by swinging the consensus conception away from diachronous regionalized glaciation (Crawford and Daily, 1971; McElhinny et al., 1974; Crowell, 1983, 1999; Eyles, 1993) towards synchronous global mega-events (Kaufman et al., 1997; Hoffman et al., 1998; Kennedy et al., 1998; Walter et al., 2000). This was, in fact, a return to earlier ideas (Mawson, 1949; Harland, 1964; Dunn et al., 1971) and it provided a possible basis for global stratigraphic correlation. These and other circumstances motivated me to undertake a systematic, regional-scale investigation of the structural geology, physical stratigraphy, U-Pb geochronology, and stable-isotope chemostratigraphy of the Otavi Group. This work, which still continues, began in earnest in 1993 and forms the basis of this guidebook. The investigation was greatly aided in its early stages by previous mapping in the study area (Martin, 1965; Frets, 1969; Guj, 1970; Porada, 1974; Hedberg, 1979; Miller 1980) and by an earlier chemostratigraphic study of the Otavi Group in the Otavi Mountains (Kaufman et al., 1991).

The purpose of the excursion is to examine the carbonates that bound the two discrete glaciogenic intervals of the Otavi Group, the Chuos and Ghaub diamictites (Martin et al., 1985; Hoffmann and Prave, 1996). Particular attention will be paid to the post-glacial “cap carbonates”, which figure prominently in the current controversy surrounding the “snowball earth” hypothesis (Kirschvink, 1992; Hoffman et al., 1998; Hoffman and Schrag, 2000, 2002; Kennedy et al., 2001; Hoffman et al., 2002). Cap carbonates are unique to Proterozoic glacial events and the two in the Otavi Group are distinct from each other as well as from other carbonates in the same succession. Moreover, many of the features that distinguish the Otavi Group cap carbonates are observed in arguably correlative cap carbonates on other cratons (Grotzinger and Knoll, 1995; Kennedy et al., 1998; James et al., 2001; Hoffman and Schrag, 2002). Cap carbonates thus appear to represent global events, with profound implications both for their origin (Hoffman et al., 1998) and for Neoproterozoic global correlation (Harland, 1964).

REGIONAL SETTING

The Otavi Group is exposed for over 700 km along strike in a Pan-African (ca 550 Ma) fold belt that rims the southwest corner of the Congo craton in northern Namibia (Fig. 1, 3). Equivalents of the Otavi Group occur extensively in the subsurface of the Etosha and Congo cratonic basins (Miller, 1997; Daly et al., 1992) and outcrop in other fold belts that circumscribe the craton (Hambrey and Harland, 1981). For example, paired glaciogenic units with distinct cap carbonates similar to those of the Otavi Group occur in the West Congo belt of Angola (Schermerhorn and Stanton, 1963) and the Irumide belt of Zambia-Shaba (Cahen and Lepersonne, 1981). Early studies of the Otavi Group centered on the Otavi Mountains mining district at the eastern plunge of the fold

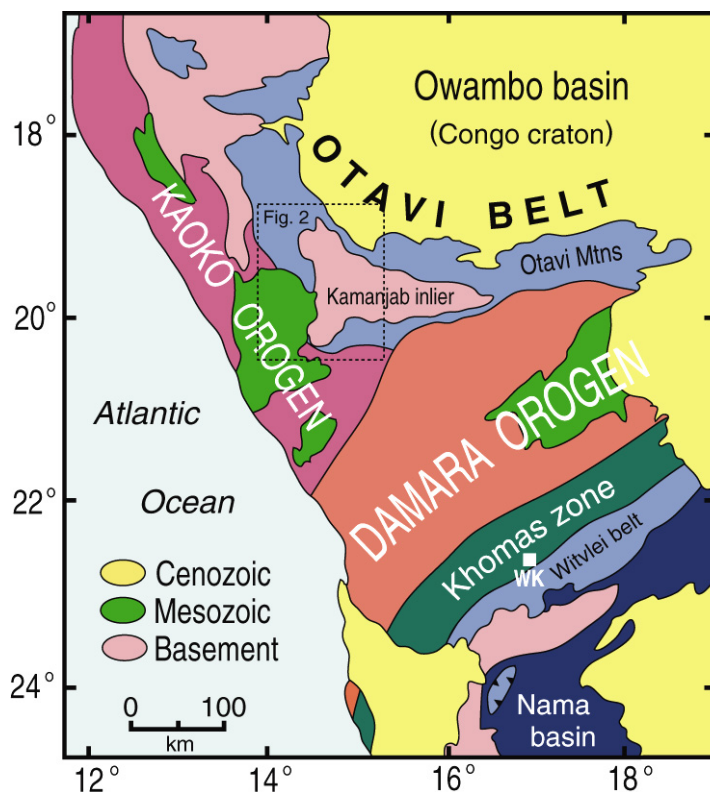


Fig. 1. Tectonic zonation of central and northern Namibia. Excursion begins and ends in Windhoek ('Wk'). Area of excursion and Fig. 2 is indicated by dashed box.

belt, but the best exposure occurs 350 km to the west, where the syntaxial “elbow” of the fold belt intersects the actively eroding coastal escarpment (Fig. 1). Here, the fold belt divides around a broad basement antiform, the Kamanjab inlier, which exposes a geon-19 (i.e., 1900-1999 Ma) metamorphic complex. This excursion is to sections on the southern and western flanks of the Kamanjab inlier (Fig. 2).

Two orthogonal orogens, the Damara and Kaoko (Fig. 1), contributed to the deformation in the Otavi fold belt. The coast-normal segment of the fold belt records minor horizontal shortening of the southern margin of the Congo craton in response to severe contraction in the Damara orogen (Hoffmann, 1987; Miller, 1983), which separates the Congo and Kalahari cratons (Fig. 1). The involvement of crystalline basement in the broad folds of the Otavi belt indicates that metamorphic temperatures at the top of the basement peaked in the field of dislocation creep for quartz, or above ~300°C. Much of the Damara orogen consists of Congo-type crust that was horizontally stretched during Otavi time, blanketed with Otavi-equivalent sedimentary strata, and then shortened (inverted) in a low P/T metamorphic facies series during the the Damaran orogeny (Henry et al., 1990) ca 560-550 Ma. The southernmost internal zone of the orogen, the Khomas zone (Fig. 1), is a south-vergent, sediment-dominated, accretionary prism, indicating that some Kalahari lithosphere was subducted northward beneath the Damara orogen (Kukla and Stanistreet, 1991). The width of subducted lithosphere was not great, for no significant magmatic arc developed. Instead, the Damara orogen was invaded by large, tabular, largely post-tectonic, syenogranites (Miller, 1983), whose age (ca 500-530 Ma) and origin remain uncertain.

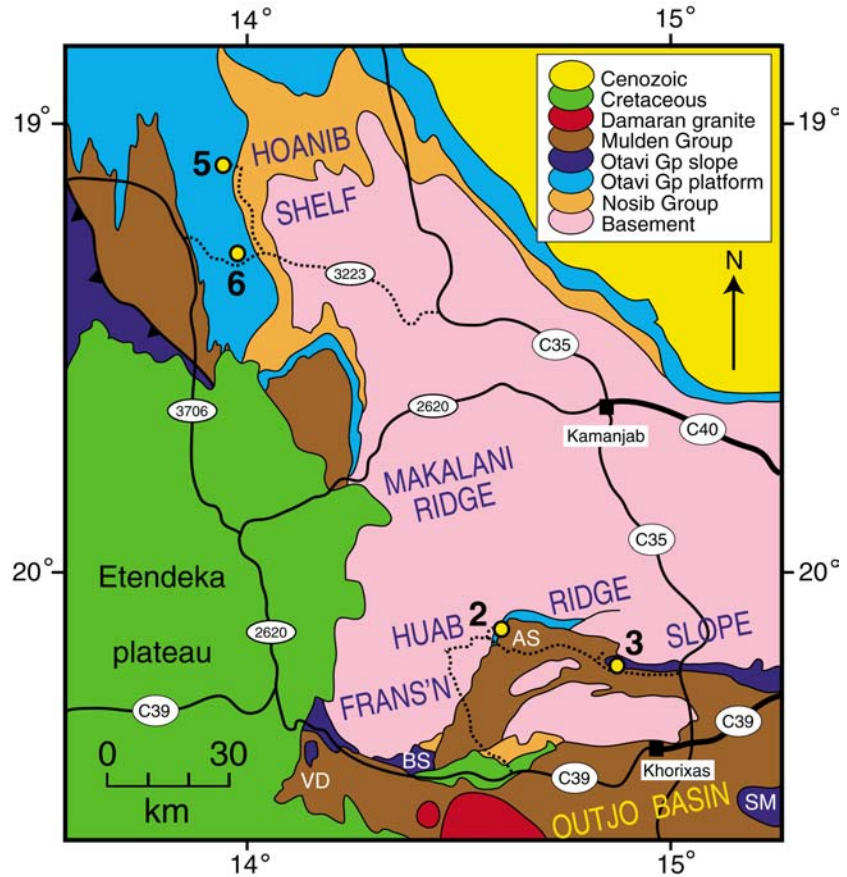


Fig. 2. Simplified geology, paleogeographic zones, and access roads around the western syntaxis of the Otavi fold belt. Daily excursion stops are shown by numbered yellow dots. AS-Achas syncline; BS-Bethanis syncline; SM-Summas Mtns; VD-Vrede domes.

North of the “elbow”, the coast-parallel segment of the Otavi fold belt borders the Kaoko semi-orogen (Hoffmann, 1987; Guj, 1970), which is the African half of the coastal orogen that separated the Congo and Rio de la Plata cratons in Gondwanaland. A long-lived, late Neoproterozoic, magmatic arc (Dom Feliciano arc) hugs the coast of southern Brazil opposite the Kaoko belt (Babinski et al., 1996, 1997). It indicates that a broad ocean was consumed beneath the coastal orogen. The Kaoko orogen is a zone of sinistral transpression, vergent toward the Congo craton (Guj, 1970; Coward, 1981). Sediment transport in foredeep clastics of the Mulden Group (Fig. 2), which overlie the Otavi Group disconformably, accords with diachronous, north-to-south closure of the coastal orogen (Stanistreet et al., 1991). U-Pb ages in Brazil imply that terminal collision at the latitude of the Otavi Group occurred ca 600-580 Ma (Babinski et al., 1996, 1997), consistent with structural studies (Coward, 1981) and the Aeromagnetic Anomaly

Map of Namibia (Geological Survey of Namibia, undated), which suggest that the Kaoko orogen is somewhat older (ca 600-580 Ma) than the Damara belt (ca 560-550 Ma).

Broadly simultaneous convergence of the Congo, Rio de la Plata and Kalahari cratons produced an unstable triple junction involving sinistral-oblique, convergence zones (the Kaoko, Damara and Gariep belts). The resulting orogenic topography gave rise to groundwater flows that arguably drove the economic Cu-Pb-Zn mineralization in the Otavi Mountains and caused pervasive chemical remagnetization of Neoproterozoic-Cambrian strata throughout Namibia (Evans, 2000). The only paleomagnetically constrained paleolatitude for the Otavi Group is $10\pm 5^\circ$ at 755 ± 25 Ma (Evans, 2000), with an apparent paleopole in the central North Atlantic, assuming that paleomagnetism of the Mbozi complex in the eastern Congo craton (Meert et al., 1995) is primary and well dated.

STRATIGRAPHIC DEVELOPMENT

Tectonic subsidence accommodating Otavi Group sedimentation resulted from roughly coast-parallel crustal stretching and subsequent thermal readjustment (Halverson et al., 2002). The azimuthal orientation of the principal strain axes is inferred from two sources of data. First, major stratigraphic cutoffs (Fig. 4) resulting from incremental crustal flexure and erosional truncation project roughly coast-normal across the Kamanjab inlier (Fig. 2). Second, paleocurrents and other paleoslope indicators were directed consistently northward (coast parallel) during pulses of dip-slope erosion and coarse clastic sedimentation in the lower and middle Otavi Group. Stratigraphic and facies relations document two distinct sources for this debris, the Huab and Makalani ridges (Fig. 3), which together were recognized on somewhat different grounds by Porada et al. (1983). Following Soffer (1998), the two ridges are provisionally attributed to footwall uplift associated with normal-sense fault systems. The fault systems are strictly hypothetical, however, because the Otavi Group was completely removed near the inferred fault lines by erosional down-cutting beneath the Mulden Group and/or the Karoo (Carboniferous) glacial surface on which the Cretaceous sandstone and flood basalt rest (Fig. 2). A different paleogeographic regime apparently existed during fluvial clastic sedimentation of the Nosib Group (Fig. 3), which preceded the Otavi Group. Paleocurrents in the Nosib Group are directed consistently southward throughout the region (Fig. 2), and indicate that the Huab and Makalani ridges did not yet exist at that time.

The recognition of two discrete glacial episodes led to the subdivision of the Otavi Group into three subgroups (Hoffmann and Prave, 1996). The Ombombo subgroup (Fig. 4) is overlain by the glaciogenic Chuos diamictite ("Varianto Formation" of SACS, 1980) with a low-angle (1.5°) unconformity, or by the Rasthof cap-carbonate sequence where the glacial deposits are absent. By convention, the diamictite or its respective cap carbonate defines the base of the succeeding subgroup. Thus, the Abenab subgroup includes the Chuos-Rasthof couple, the mixed clastics and carbonates of the Gruis Formation, associated with renewed crustal stretching on the Otavi platform, and the Ombaatjie Formation, which was accommodated by rapid, post-rift, thermal subsidence. The Abenab subgroup spans the "rift-drift" transition on the Otavi platform, although stretching continued in the Outjo basin to the south. The Ombaatjie Formation is overlain disconformably by the Ghaub diamictite, or by the Maieberg cap-carbonate sequence where the diamictite is absent. The Tsumeb subgroup includes the Ghaub-Maieberg couple and the thick, shallow-water, Elandshoek-Hüttenberg carbonate platform. The top of the platform is a regional disconformity, locally with spectacular map-scale paleokarst having >200 m of local relief (Frets, 1969, p. 103), which is overlain by collisional foredeep clastics of the Mulden Group. South of the platform, crustal stretching was more severe and continued through the Ghaub glaciation (at least). On the Fransfontein slope (Fig. 3), the Abenab and Tsumeb subgroups are represented by slope and basin facies exclusively, and are strongly condensed (partly due to submarine mass wasting) relative to equivalent sections on the platform correlated isotopically.

Ombombo Subgroup

The Ombombo subgroup (Hoffmann and Prave, 1996) consists of mixed carbonate and clastic strata that lie conformably on the Nosib Group and are truncated with a low-angle (1.5°) erosional unconformity beneath the Chuos glacial surface. It is most extensively exposed on the Hoanib shelf north of the Makalani ridge (Fig. 3), where it forms a wedge that reaches 1500 m in thickness 200 km north of the feather edge. Three mappable

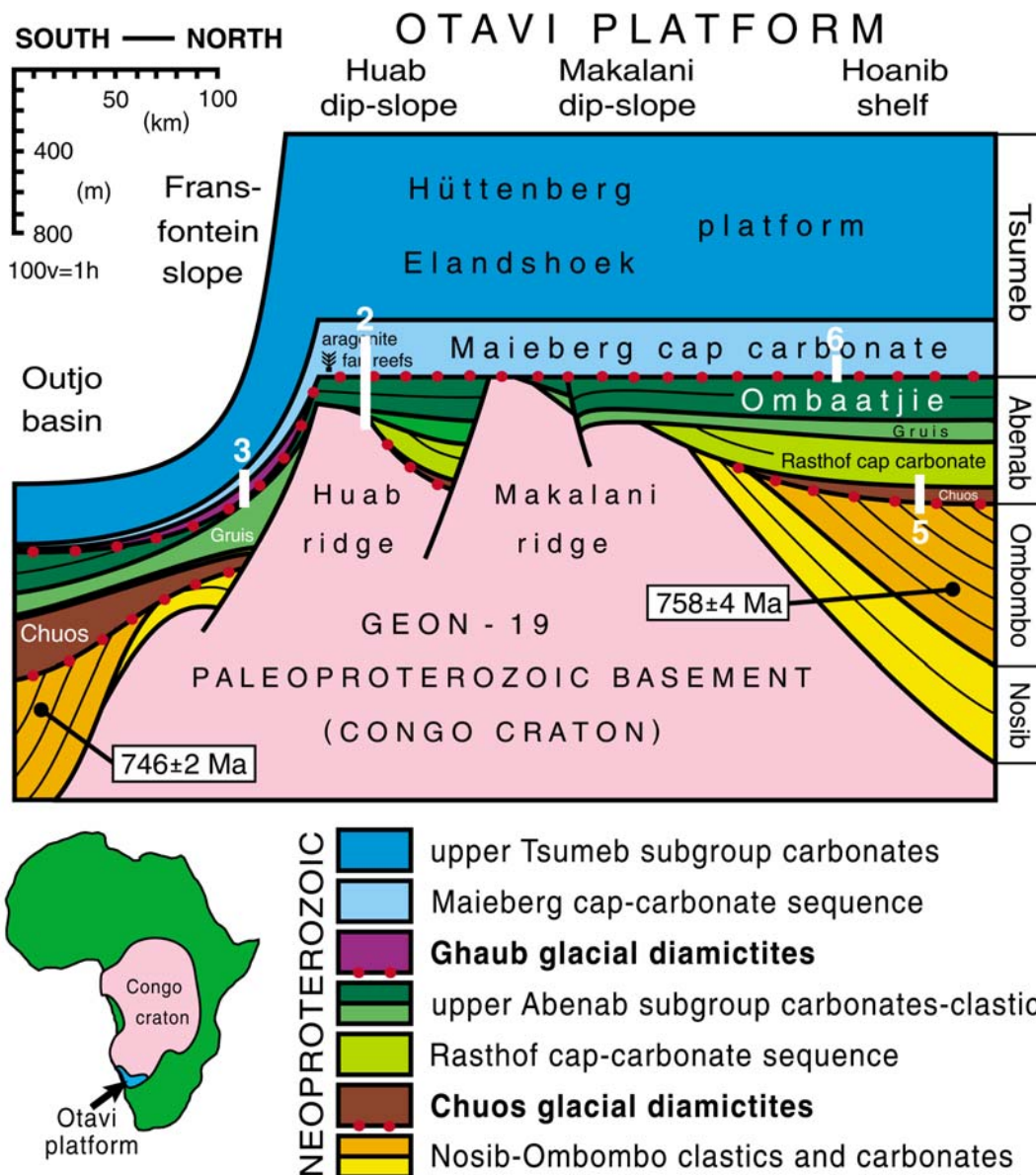


Fig. 3. Coast-parallel stratigraphic cross-section of the Otavi Group based on systematic mapping and measured sections on the western and southern flanks of the Kamanjab inlier (see Fig. 2). Vertical white bars indicate the approximate projections of the Excursion sections onto the cross-section.

stratigraphic units are informally recognized (Fig. 4), a lower mixed carbonate and fine clastic unit (“Beesvlaakte Formation”), a middle carbonate-dominated unit (“Devede Formation”) and an upper clastic-dominated unit (“Okakuyu Formation”). A prominent *Tungussia*-type stromatolite biostrome overlain by deeper-water allodapic (turbiditic) beds (“*Tungussia* member”) occurs at the base of the Okakuyu Formation and a similar stromatolite with coarse oolite appears at the top of the same formation in sections distal from the Makalani ridge. Sedimentary facies imply that deposition occurred on a north-dipping ramp that was subject to episodic uplift and cannibalistic erosion in the area of the Makalani ridge. Northward-fining tongues of coarse clastic debris, derived from cover strata and the basement metamorphic complex, occur in proximal areas of the Ombombo Group wedge. The clastic tongues are hosted by varicolored cherty dolostone, dominantly grainstones and stromatolites. The dolostone consists of shoaling-upward, peritidal parasequences with a mean thickness of 15 m. In the Devede Formation, clastic incursions from the south appear in the transgressive systems tracts of the parasequences. Characteristic pale pinkish stromatolite biostromes up to 70 m thick are composed of the form “genus” *Tungussia*, with *Jacutophyton* as a local variant. *Tungussia* is a columnar type with exuberant branching that is strongly divergent, even downward propagating; *Jacutophyton* is characterized by central vertical columns with acute conical internal laminae and annular petal-like branching. A practised eye is needed because the lamination defining the Ombombo stromatolites

is quite subtle. A tip: the *Tungussia* biostromes look at first glance like an oligomictic carbonate-pebble conglomerate! The upper Ombombo subgroup (Okakuyu Formation) is a stack of coarsening-upward clastic parasequences, culminating in chert-dolomite±volcanic- and/or basement-clast conglomerates. In the type section, a thick *Tungussia* stromatolite biostrome associated with coarse-grained oolite occurs at the top of the Okakuyu Formation, directly beneath the Chuos diamictite. The Ombombo subgroup does not occur on the Makalani or Huab ridges, or in the Otavi Mountains (Hoffmann and Prave, 1996), but is sporadically exposed in the Outjo basin (Fig. 3). The Outjo basin did not yet exist as such in Ombombo time and the sedimentary facies there are similar to those on the Hoanib shelf.

The depositional age of the Ombombo subgroup is directly constrained by single-crystal U-Pb zircon ages determined by thermal ionization mass spectrometry (TIMS). A 15-cm thick tuff in the middle Ombombo subgroup (upper Devede Formation) on the Hoanib shelf gives a preliminary age of 758 ± 4 Ma (S.A. Bowring unpublished data), indistinguishable from the age of 756 ± 2 Ma (Hoffman et al., 1996) obtained for a quartz-syenite body that intrudes the Nosib Group and nonconformably underlies the Abenab subgroup in the Outjo basin 200 km to the southeast. Significant accumulations of mixed mafic-felsic lava and tuff (Naauwpoort Formation) occur in the Outjo basin (Frets, 1969; Miller, 1980) and our work suggests that they belong almost exclusively to the Ombombo subgroup (tuffs also occur at or near the top of both the Chuos and Ghaub diamictites). Felsic lava and ash flows in the Summas Mountains (Miller, 1980) give ages of 747 ± 2 and 746 ± 2 Ma, respectively (Hoffman et al., 1996), and recent work confirms their assignment to the Ombombo subgroup and position unconformably beneath the Chuos diamictite in the same area. Volcanic pebbles in conglomerate near the top of the Ombombo subgroup on the Hoanib shelf could be derived from equivalents of the Naauwpoort Formation, but only undateable(?) mafic pebbles are present.

Carbonates of the Ombombo subgroup are strongly enriched in ^{13}C (Fig. 4), with $\delta^{13}\text{C}$ rising gradually from +4.0 to +6.0 per mil (VPDB) through the 400-m-thick Devede Formation on the Hoanib shelf (Fig. 4). Directly beneath the Chuos diamictite, $\delta^{13}\text{C}$ declines to +3.0 per mil on the Hoanib shelf and -1.0 per mil in the Outjo basin. Thus, the Chuos glaciation conforms with the general observation that Neoproterozoic glacial episodes follow long periods of high inferred organic fractional burial (Kaufman et al., 1997), terminated by steep declines in $\delta^{13}\text{C}$ that lead glaciation (Schrag et al., 2002; Halverson et al., 2002).

Chuos diamictite

Deposits from the Chuos glaciation are thin or absent on the Huab and Makalani ridges, but wedge in to the south and north (Fig. 3), reaching over 300 and 1000 m thickness in the Summas and Steilrand mountains, respectively. Massive to weakly stratified diamictite is the predominant lithology in most sections, locally with pebbly sandstone (outwash), laminated siltstone with or without dropstones, and iron-formation. The diamictites are derived from basement metamorphic and Nosib-Ombombo cover rocks in varying proportions. The diamictite matrix is invariably wackestone, maintaining a continuous spectrum of grain sizes from meter-scale boulders downwards through five orders of magnitude. The silicate-carbonate ratio in the matrix and clast population covaries. The matrix is commonly ferruginous and the variation in colour of different diamictite units, either greenish-grey, black, reddish-brown, or tan, is a function of redox and lithology. Ferric iron content commonly increases

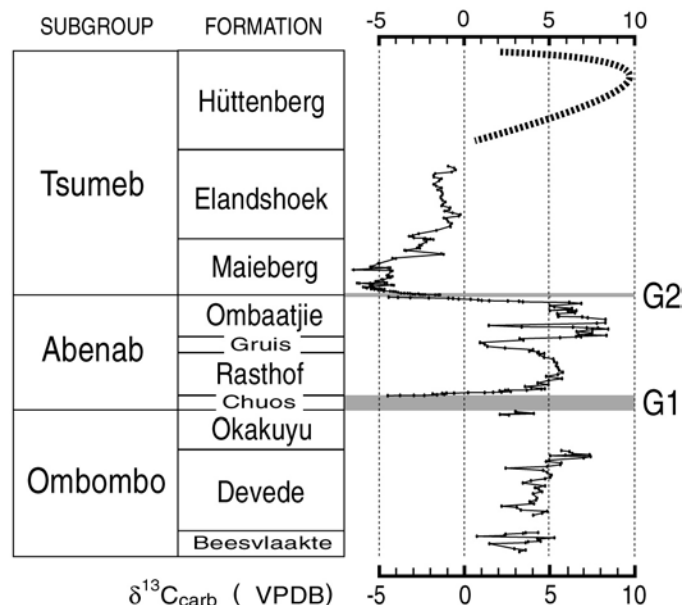


Fig. 4. Stratigraphic nomenclature and a representative carbon isotopic profile for the Hoanib shelf. The upper Tsumeb subgroup profile is from Kaufman et al. (1991) and unpublished data. Note negative anomalies associated with the Chuos (G1) and Ghaub (G2) glaciations.

toward the top of the formation, but the significance of this is clouded by secondary mobilization: hematite is concentrated on cleavage planes and the basal Rasthof cap dolostone is reddened. Both the base (even where not erosional) and the top of the glacial interval are sharply defined, a characteristic of Neoproterozoic glacials generally (Hoffman and Schrag, 2000), and this implies that glacial episodes began and ended abruptly. Dolostones directly beneath the glacial deposits are intensely shattered and silicified in many platformal sections, and large slabs of dolostone are in places only slightly dislodged from their source. At Omurirapo (Excursion Day 5), on the Hoanib shelf, the basal Chuos erosion surface has 385 m of local relief, overlapped by diamictite. The paleoscarp is localized by subcropping, resistant, conglomeratic sandstones (Okakuyu Formation) in the upper Ombombo subgroup, which dipped 1.5° to the north.

A glacial origin for the Chuos Formation is indicated by characteristic diamictites, observed nowhere else in the Ombombo or Abenab subgroups, by stones with multiple striations found within diamictite, and by rare but excellent dropstones in laminated siltstone. Most of the Chuos Formation was deposited under ice, but the degree to which this occurred above or below sea level has not been determined. The wedge-shaped geometry of the Chuos “basins” of preservation probably reflects continuing footwall uplift and dip-slope rotation due to coast-parallel crustal stretching that initiated in early Ombombo time. The low-angle unconformity at the base of the diamictite might signify a pulse of deformation around the time of the glacial onset, or alternatively represents a long break in sedimentation while deformation continued at a steady rate. The latter interpretation (Hoffman, 2000) would be consistent with the snowball Earth scenario, in which temperatures were too low to generate significant precipitation for millions of years before accumulated atmospheric CO₂ drove temperatures close to melting (Caldeira and Kasting, 1992). Accordingly, the diamictite would represent only the final stage of the glacial episode, with the sub-Chuos hiatus representing the lion’s share of the time interval in the snowball state when it was too cold and dry for dynamic continental ice sheets.

The only direct age constraint on the Chuos glaciation is that it began well after 746±2 Ma, the age of rhyolite ash-flow tuff (Naauwpoort volcanics) in the Summas Mountains (Hoffman et al., 1996), which is stratigraphically separated from the Chuos diamictite by up to 720 m of upper Ombombo mixed carbonates and clastics. This constraint permits proposed correlations with the Sturtian (Australia), Rapitan (Canada), Elbobreen (Svalbard), Tsagaan Gol (Mongolia), Gubrah (Oman), or Blaubecker (central Namibia) glaciations (Shields et al., 1997; Kennedy et al., 1998; Brasier et al., 2000; Walter et al., 2000; Hoffman and Schrag, 2002). It potentially conflicts with a proposed correlation with the Kaigas diamictite in the Gariep belt of southern Namibia, based on a Pb-Pb zircon age of 741±6 Ma for the Rosh Pinah volcanics (Frimmel et al., 1996). Either the Kaigas diamictite is older, not younger (Frimmel et al., 1996), than the Rosh Pinah, or it is not correlative with the Chuos diamictite, or the 720 m of post-Naauwpoort Ombombo strata were deposited very rapidly.

Rasthof cap-carbonate sequence

The Rasthof cap-carbonate sequence invariably overlies the Chuos diamictite or its equivalent erosion surface where the diamictite is absent (Fig. 3). The diamictite-dolostone interface is a knife-sharp depositional contact, without evidence of reworking, exposure, or significant hiatus. The top of the “cap-carbonate sequence” is defined (Hoffman and Schrag, 2002) at the first subaerial exposure surface. In the Hoanib basin, the sequence is typically 200-240 m (maximum 355 m) thick. This is at least one order of magnitude greater than the average parasequence thickness (i.e., stratigraphic separation between successive exposure surfaces) in the Ombombo or upper Abenab subgroups. Both the Rasthof and Maieberg cap-carbonate sequences are essentially single parasequences that are one to two orders of magnitude thicker than the proximal stratigraphic norm. A similar pattern exists in many Neoproterozoic successions world-wide (Hoffman and Schrag, 2002). According to the snowball hypothesis, this reflects two factors (Hoffman et al., 1998; Halverson et al., 2002). On the one hand, a large amount of tectonic subsidence (and elsewhere uplift) occurred during millions of years of deep freeze, when the average sedimentation (erosion) rate was very low, thereby creating accommodation space for large volumes of sediment following post-glacial sea-level rise. On the other hand, an intense post-glacial weathering regime supplied alkalinity (most rapidly from carbonate weathering) that drove carbonate sedimentation, and terrigenous material (Hoffman et al., 1998). In the Otavi Group, the alkalinity flux prevailed. In the Otavi Mountains, the Berg Aukas Formation (SACS, 1980; Hoffman and Prave, 1996) is equivalent to the Rasthof.

On the Makalani dip slope, the Rasthof thins progressively to a feather edge due to erosional truncation beneath the overlying Gruis Formation (Fig. 3), which cuts down section from north to south. This is easily demonstrated because of the “layer-cake” internal stratigraphy of the Rasthof north of the Makalani ridge. At the base is a unit of dark grey dolomitic limestone that is characterized by abiotic, mm-scale lamination. This unit thickens southward through the addition of cm-scale allodapic layers, typically graded with clastic dololomite tops. The top of the abiotic unit is marked by an abrupt transition to sublittoral microbialaminite, which continues unbroken for >150 m. This astounding interval of dark to medium grey dolostone was deposited in a strictly sublittoral environment characterized by continuous and perpetual, thick, rubbery, microbial mats. The microbial lamination is ubiquitously convoluted. Slumping may account for some of the contortion, but much appears to result from azimuthal growth expansion. This is inferred from abundant soft-sediment “thrust-ramp anticlines” with no preferred azimuth of vergence. Distinctive “roll-up” structures show that the mats were coherent but pliable, and irregular networks of syndepositional breccia suggest fluid or gas escape. Near the top of the sequence, the microbial lamination becomes indistinct and passes imperceptibly into fine epiclastic dolostone that coarsens to dolarenite with supratidal tepees (Kendall and Warren, 1987) at the top. The epiclastic unit is typically 20-50 m thick.

The Rasthof $\delta^{13}\text{C}$ profile on the Hoanib shelf is distinctive and regionally reproducible (Fig. 4, 14). The abiotic basal unit rises rapidly from -4.5 to -2.0 per mil in the first meter and then more gradually to 0 per mil at the top. The curve rises rapidly once again where the lamination becomes microbial and then levels off around $+5$ per mil through the thick microbialaminite interval, before declining one per mil in the upper grainstones. The abrupt rise in $\delta^{13}\text{C}$, systematically coincident with the local substrate change (abiotic to microbial), irrespective of the height where it occurs (2-70 m), suggests that the high value of $+5$ per mil for the microbialaminite records local conditions in a restricted basin. If the isotopic shift was global, only chance could account for its consistent correlation with the regional microbial “invasion”.

Erosional truncation of the Rasthof by Gruis Formation conglomerate was first documented by Soffer (1998) on the Huab dip slope (Fig. 3) on Tweelingskop 676 farm on the Huab River (see Excursion Day 2). Some 285 m of Rasthof dolostone is truncated beneath the sub-Gruis unconformity in a north-south distance of 4 km, giving a mean angle ~ 4 degrees for the Rasthof-Gruis discordance at this location. The abiotic basal unit with $\delta^{13}\text{C} \leq 0$ per mil is missing in most sections on the Huab ridge, implying that the ridge had topography at the end of the Chuos glaciation that was overlapped by the lower Rasthof. Tweelingskop is one of the few locations on the Huab ridge where Chuos diamictite is locally preserved beneath the Rasthof. There, large-scale debris flows characterize the Chuos-Rasthof transition. Cannibalistic debris flows also occur in the upper Rasthof on the Huab dip slope, and they contain 30-50% fibrous isopachous cement. As a test of proposed steep $\delta^{13}\text{C}$ gradients with depth in Neoproterozoic oceans (Grotzinger and Knoll, 1995; Kennedy, 1996), we measured $\delta^{13}\text{C}$ in micro-sampled profiles of cements and clasts (both now dolomite), on the assumption that the clasts originated upslope from the cements. No significant (>0.5 per mil) variation was found; both components are uniform around $+5$ per mil.

South of the Huab ridge, dark-coloured Rasthof dolostone lies directly on crystalline basement in proximal sections (Fransfontein slope) and on Chuos diamictite distally (Outjo basin). The Rasthof thins rapidly downslope (although evidence of submarine mass wasting exists throughout the stratigraphic column in slope sections, making stratigraphic reconstruction perilous) and consists mainly of allodapic beds, including debris flows with slabs of characteristic Rasthof microbialaminite. Starved ripples of sandstone indicate west-southwest-directed contour currents. $\delta^{13}\text{C}$ profiles in proximal slope sections resemble those on the Huab ridge, but the basal unit with values well below 0 per mil reappears in distal sections.

Upper Abenab subgroup

The upper Abenab subgroup consists of the Gruis and Ombaatjie Formations (Fig. 3), which are correlative with the Gauss and Auros Formations, respectively, in the Otavi Mountains (SACS, 1980; Hoffmann and Prave, 1996). The Gruis Formation marks the last major crustal stretch affecting the Huab ridge, and represents a period of uplift and back-rotation of the Makalani ridge as well. High on both the Huab and Makalani dip slopes, the Gruis Formation contains up to 150 m of alluvial fanglomerate, incised into the basement complex. Downslope (on both ridges), the clastics become rapidly finer grained and are intercalated with tan-coloured, supratidal dolostone characterized by ubiquitous “tepees” (Kendall and Warren, 1987), the trademark sedimentary structure of the Gruis Formation. On the Hoanib shelf, the Gruis is represented by 80-200 m of tan and grey dolostone, mainly peritidal microbialaminites and grainstones, with marly intervals as the distal equivalents of the dip-slope clastics. Gruis dolostones are strongly enriched, with $\delta^{13}\text{C}$ values for pure carbonates averaging +7 per mil. It is in Gruis time that the Otavi platform margin was fully established. South of the Huab ridge, the formation consists of 10s to 100s of meters of strictly bathyal, green argillite, tan dolostone allodapic beds and debris flows, and quartz sandstone turbidites.

On the Otavi platform (Fig. 3), the Gruis-Ombaatjie transition marks a change to more regionally uniform subsidence and a simultaneous increase in apparent subsidence rate. The average parasequence thickness changes abruptly from <5 to ~25 m. The lower half (~100 m) of the Ombaatjie Formation is dominated by dark grey, cliff-forming limestone, and the upper half by more dolomitic, less resistant strata. It consists of a weakly retrogradational stack of eight or so parasequences (Halverson et al., 2002), the lower half of which are dominated crossbedded intraclast grainstone. On the upper Makalani dip slope, the lower parasequences are missing and where they appear on the lower slope they contain tongues of mature quartz sandstone. Similar relations are observed on the Huab dip slope (where the sub-Mulden karst limits the availability of sections). These relations suggest that the lower Ombaatjie has an onlap relationship with respect to residual topography inherited from the previous crustal extension. An antithetic fault on the Makalani dip slope was apparently active in latest Ombaatjie time and the top of the ridge was stripped to basement during the Ghaub glaciation (Fig. 3), implying a final episode of back-rotation presumably related to crustal stretching in Outjo basin at that time. $\delta^{13}\text{C}$ values through the first six parasequences hold steady around +5 per mil on the Huab dip slope and +7 per mil on the Makalani dip slope and Hoanib basin, presumably reflecting a significantly restricted inner shelf (Halverson et al., 2002). Through the final two parasequences, however, $\delta^{13}\text{C}$ in all sections declines steadily before flattening out around -5 per mil, a 10 per mil descent over a stratigraphic interval of ~30 m, estimated from a thermal subsidence model to represent ~0.5 myr (Halverson et al., 2002). Similar large drops in $\delta^{13}\text{C}$ are observed in advance of the Elatina (Australia), Ice Brook (Canada), Port Askaig (Scotland), Elbobreen (Svalbard) and other late Neoproterozoic glacial episodes (Halverson et al., 2002; Hoffman and Schrag, 2002). Schrag et al. (2002) propose an explanation for these remarkable negative anomalies and the positive values that long precede them, within the context of a climatic destabilizing mechanism involving steady-state atmospheric methane buildup.

South of the Huab ridge, 60-300 m of allodapic grey dolostone (fine debris flows and grainflows) occur between the green argillite-dominated interval assigned to the Gruis Formation and the much coarser diamictites of the Ghaub glaciation (Fig. 3). This unit is logically correlated as a slope and toe-of-slope facies of the Ombaatjie platform. However, $\delta^{13}\text{C}$ values scatter between -4 and 0 per mil throughout (Halverson et al., 2002). Positive $\delta^{13}\text{C}$ values equivalent to Ombaatjie parasequences 1-6 on the platform are limited to the “Gruis” on the slope. This may be explained in three ways, not equally probable. The first is that the negative values in the deep water sections indicate a contemporaneous 5-9 per mil difference in $\delta^{13}\text{C}$ between surface and deep water (versus 2-3 per mil difference in the modern and Mesozoic-Cenozoic oceans). This explanation can be discounted because the negative values come from grains that originated up slope, including clasts of ooid grainstone that must represent the surface ocean. The second explanation is that the allodapic unit is correlative with parasequences 7 and 8 on the shelf, when surface-water $\delta^{13}\text{C}$ had declined <0 per mil. However, this explanation is unsatisfactory because it provides no rationale for the prominence down slope of only those two parasequences. The third explanation is that the allodapic beds were shed downslope as a consequence of sea-level fall associated with the Ghaub glaciation that exposed the platform. In this case, they could be broadly correlative with 30 m of recrystallized dolarenite, tentatively interpreted as aeolianite, that lies disconformably above parasequence 8 and below the Maieberg cap carbonate on the Huab ridge at Tweelingskop (see Excursion Day 2). The aeolianite has $\delta^{13}\text{C}$ values of -3 per mil (Halverson et al., 2002). The slope might have been a sedimentary bypass zone during earlier Ombaatjie time, or

alternatively, earlier Ombaatjie equivalents are contained within the mixed deepwater clastics and carbonates tentatively assigned to the “Gruis”, with the clastics supplied by intrabasinal highs resulting from continued (syn-Ombaatjie) crustal stretching in the Outjo basin. During the Ghaub glaciation, tectonic subsidence slowly lowered the platform enabling it to accommodate the thick Maieberg cap-carbonate sequence upon post-glacial sea-level rise.

Ghaub diamictite

Around the “elbow” of the fold belt, the Ghaub diamictite is best developed on the Fransfontein slope (Fig. 3), where it is continuous and 30-180 m thick. It is composed overwhelmingly of Abenab-derived carbonate debris (one basement clast per outcrop is the norm), but the limestone/dolomite ratio (of clasts or matrix) is highly variable. Notable in the clast population are coarse-grained ooid grainstone, botryoidal stromatolite, and isopachous cementstone (see Excursion Day 3). The first two are standard lithofacies of windward shelf edges and the third closely resembles cement in debris flows of the upper Rasthof on the Huab ridge. Much if not most of the debris is therefore locally derived, not transported across the platform. Rare basement clasts could come from the Makalani ridge. The slope-facies diamictite consists mostly of massive to graded debris flows, but the lower part and the top of the unit are characterized by thin-bedded allodapic carbonate studded with polymictic dropstones (see Excursion Day 3). Outwash is virtually absent. Superb dropstones, some with soft-sediment, impact-generated folds (Hoffman and Schrag, 2002), constitute strong lithological evidence for glaciation (Condon et al., 2002). The Ombaatjie-Ghaub transition on the slope is an abrupt change from comparatively fine, oligomictic (intraformational) debris flows to variably ferruginous allodapic beds with dropstones and polymictic debris flows with outsize clasts. The abruptness of the transition at paleodepths below any ice-grounding line implies that glaciers appeared suddenly. Less obvious is whether continental ice sheets or “sea glaciers” were involved. Sea glaciers on a snowball Earth would flow equatorward due to the steady-state difference in sea-ice thickness from pole to equator maintained by a weak hydrologic cycle (Warren et al., 2002). The bedded dropstone member at the top of the Ghaub is present in virtually all slope sections, never more than a few meters thick, and presumably records the final glacial collapse. In a number of sections, this unit is associated with layers of volcanic ash up to 2.8 m thick, possibly released from melted ice. Sadly, they do not contain primary zircons. Less common in the Ghaub are intervals of very fine-grained, even-textured, faintly laminated siltstone up to 10s of meters thick, and beds of well-sorted, well-rounded, medium-grained, quartz sandstone. These uncommon strata are interpreted as subaqueously deposited loess and wind-blown sand. Kennedy et al. (2001) claim to have sampled carbonate cements precipitated from seawater during the Ghaub glaciation, but I am unable confirm the existence of such cements.

On the Otavi platform, the Ghaub is limited around the “elbow” of the fold belt to small patches of diamictite generally <3 m thick, tucked beneath the Maieberg cap-carbonate sequence (see Excursion Day 6). In most sections, the basal member of the Maieberg, the Keilberg “cap dolostone”, directly overlies the Ombaatjie platform. Where present, the diamictite shows no evidence of having been eroded before the Maieberg was deposited. There is no lag conglomerate, no channels, and no sign of significant hiatus. The paucity of diamictite on the platform reflects non-deposition, not subsequent erosion. In the Otavi Mountains, however, up to 200 m of Ghaub diamictite does occur extensively on the Otavi platform (Hoffmann and Prave, 1996) and the proportion of extrabasinal clasts is greater there as well. In the Summas Mountains, the diamictite is again commonly missing, but an angular unconformity (locally up to 35°) occurs at the Ombaatjie-Maieberg contact. This indicates either that the pulse of tectonic block rotation occurred coincident with glaciation in the Outjo basin, or alternatively that tectonic activity was continuous and the stratigraphic localization of the angular discordance marks a long hiatus during glaciation when little or no sedimentation occurred in the basin.

Given its modest thickness and stratigraphic impersistence, the Ghaub glaciation has been correlated very widely, mainly on account of its distinctive cap-carbonate sequence and the bounding isotopic profiles. It is equated with the Blässkranz and Numees diamictites in the Witvlei and Gariep belts on the northern and western margins respectively of the Kalahari craton (Fig. 1), and more tentatively with the Marinoan and Ice Brook glaciations in Australia and Canada, respectively (Kennedy et al., 1988; Walter et al., 2000; Hoffman and Schrag, 2002). Although glacial deposits of this age are locally very thick (350-2000 m) and rich in mudrock like temperate proglacial environments (McMechan, 2000a,b), their volume overall is pretty puny given robust paleomagnetic evidence for equatorial glaciation at sea level lasting through multiple geomagnetic reversals (Embleton and

Williams, 1986; Schmidt et al., 1991; Schmidt and Williams, 1995; Sohl et al., 1999; Evans, 2000). Preiss (2000) suggests that the “low-lying cratonic region was never overridden by a continental ice sheet” during the Marinoan glaciation in South Australia, consistent with evidence from the Ghaub glaciation in Namibia. This is the converse of the “loophole” climate model for low-latitude glaciation, in which all continents are heavily glaciated but the tropical ocean remains ice free (Hyde et al., 2000; Runnegar, 2000).

Maieberg cap-carbonate sequence

The Maieberg cap-carbonate sequence is a single transgressive-regressive depositional sequence that is 300-400 m thick on the Otavi platform (Fig. 3). On the Fransfontein slope, the well-developed exposure surface that defines the top of the sequence disappears, but the isotopic anomaly that accompanies the sequence is condensed by more than an order of magnitude down to 20-40 m. The transgressive tract of the Maieberg cap-carbonate sequence is a distinctive pale, flinty, laminated dolostone on the Otavi platform (Fig. 3), defined as the Keilberg member (Hoffmann and Prave, 1996) or Keilberg “cap dolostone”. The diamictite-dolostone contact is sharp, flat, and lacks karst, lag, or other evidence of exposure or significant hiatus. The Keilberg cap dolostone is 10-20 m thick on the Hoanib shelf but swells to 50-75 m over the Makalani and Huab ridges. Its top in both areas is a marine flooding surface overlain by pink allodapic marly limestone. On the Huab ridge (see Excursion Day 2), the Keilberg consists of large, contiguous, broadly-arched stromatolites with invariably vertical, tube-like or sheet-like structures defined by pockets of meniscus-laminated micrite and/or silica cement (Hegenberger, 1987). This “quartz-cluster dolomite”, as it is called in the Otavi Mountains, is remarkably similar to the presumed correlative lower Noonday cap dolostone near Death Valley, California (Cloud et al., 1974; Wright et al., 1978), as well as to the Bildah cap dolostone of the Witvlei Group in central Namibia (Hegenberger, 1987, 1993; Grotzinger and Knoll, 1995) and the Bloeddrif cap dolostone of the Gariiep Group in southern Namibia (Fölling and Frimmel, 2002). Strong recrystallization renders the tube-like structure enigmatic in this platform-margin facies (compare Hoffman et al., 1998a; Kennedy et al., 2001).

The tube-like structures are much better preserved on the Hoanib shelf (see Excursion Day 6). There, the Keilberg member consists of pale, tight, fine-grained dolostone with ubiquitous, small-scale, hummocky cross-lamination. The primary texture is micro- to macro-peloidal but is typically obscured by recrystallization. Beginning ~1.0 m above the base is an interval ~3.0 m in thickness composed of large, laterally coalesced, muffin-shaped stromatolites (see Excursion Day 6). The stromatolites begin at nodes spaced 1-2 m apart and expand upward into coalescence at a similar height above their base. Internally, the stromatolites consist of two components: vertical tubular infillings of dolomicrite with distinct laminae that curl up at the edges like a meniscus, and a honeycomb of vertical, intersecting partitions that bound the filled “tubes” and which in vertical section present indistinct but strongly arched laminations that must have been stabilized microbially. In such sections, the microbial partitions appear deceptively as normal, non-branched columns with extreme height to width ratios. But in fact it is the “meniscus” pockets that are subcircular in plan view, filling pits in a lattice of microbial ridges. The “tubes” occur strictly within stromatolites, not in the hummocky cross-laminated host sediment. They do not occur at the base of the cap dolostone, contrary to expectation if the tubes originated by methane escape from glacial-age permafrost beneath the cap dolostone (Kennedy et al., 2001). Based on study of analogous structures in correlative cap dolostones in the Witvlei and Gariiep groups in Namibia and the Ice Brook cap dolostone in Western Canada (James et al., 2001), as well as the in Keilberg member, Hoffman et al. (2002) interpret the “tubes” as developing incrementally during stromatolite accretion, with little synoptic relief despite their extreme vertical “inheritance”. Locally in both the Keilberg and Ice Brook cap dolostones, the microbial ridges are parallel, as opposed to intersecting, and the meniscus pockets form parallel vertical sheets instead of tubes. This variant at least is difficult to account for by means of gas escape.

Another enigmatic primary structure unique(?) to cap dolostones appears in the middle Keilberg member—spaced antiformal cusps falsely referred to as “tepees” (see Excursion Day 6). Unlike conventional tepees (Kendall and Warren, 1987), the cusps are parallel at any horizon rather than polygonal, and they are not associated with vadose cements or other indicators of subaerial exposure. The cusps of well developed “tepees” in the Ice Brook cap dolostone (James et al., 2001) were clearly influenced if not built by (storm) wave action (Hoffman and Schrag, 2002). As hurricane intensity scales with tropical sea-surface temperature (Emmanuel, 1999), the ultra-greenhouse

aftermaths of snowball episodes should be characterized by “hypercanes”, which may have contributed to the formation of pseudo-tepees and other structures (hummocky cross-lamination, reverse-graded peloids) characteristic of cap dolostones.

The marine flooding surface at the top of the Keilberg member is overlain by 200-300 m of mainly pinkish allodapic limestone. The lower part of this interval is recessive and consists of limestone-marl rhythmite (see Excursion Day 6). Higher up, the limestone is quite pure and large-scale hummocky cross-bedding is observed. The final 100-150 m of the sequence is typically dolostone, at first allodapic and thin-bedded like the underlying limestone, and then more massive grainstone that coarsens upward to a heavily silicified exposure surface, overlain by multitudinous tepee cycles of the lower Elandshoek Formation (Fig. 3).

The remarkable $\delta^{13}\text{C}$ negative excursion (Fig. 4, 18) associated with the Maieberg sequence (Hoffman et al., 1998) has been reproduced in detail in sections up to 350 and 120 km apart, parallel and normal to the platform margin respectively, and closely similar excursions occur in the Buschmannsklippe, Tsabisis and Bloedrif cap-carbonate sequences of the Kalahari craton (Fölling and Frimmel, 2002; and the author’s unpublished data). The lower half of the Keilberg member (Fig. 19) hovers close to -3 per mil while the upper half descends to -4.5 per mil (see Excursion Day 6). There is an abrupt drop to near -5.3 per mil in the limestone-marl rhythmites and then a slow rise to between -2 and 0 per mil at the top of the sequence.

On the Fransfontein slope and Outjo basin, the entire Tsumeb subgroup is composed of allodapic dolomite and derived slump breccia. It is not possible to recognize a sequence boundary equivalent to the Maieberg-Elandshoek exposure surface on the platform, but $\delta^{13}\text{C}$ profiles suggest that the entire Maieberg equivalent section is only 20-40 m thick (Fig. 10). Although Hoffmann and Prave (1996) extended the Keilberg member to the Fransfontein slope, the primary facies differs from that on the platform. Allodapic dolostone occurs in place of hummocky cross-laminated storm deposits; stromatolites and tube-like structures are absent. A continuous zone ~ 1.0 m thick close to the base contains sub-horizontal sheet-cracks filled by isopachous sea-floor cement, now composed of dolomite or silica. These cements have been attributed to anaerobic methane oxidation (Kennedy et al., 2001), but neither the cements nor the cement-rich zone is enriched in ^{12}C relative to background strata, contrary to methane cold-seep carbonate cements (e.g., Kauffman et al., 1996).

Upper Tsumeb subgroup

On the Otavi platform, the upper Tsumeb subgroup (Elandshoek and Hüttenberg Formations) consists of 600-1600 m of cyclic, shallow-water, cherty dolostone, with shale intercalations above 1050 m (King, 1994). At the base is ~ 60 m of pinkish dolostone, composed of approximately twenty peritidal parasequences dominated by teeped microbialaminite. This is followed by 400-700 m of similar-scale dolostone parasequences dominated by cherty grainstone. The Elandshoek-Hüttenberg boundary is defined (SACS, 1980) at the first of a set of distinctive silicified stromatolite layers (“*tuten*”). The stromatolites are pseudo-columnar (laterally-linked) with a synoptic “egg-carton” morphology. The formation boundary appears to have little significance in terms of sequence stratigraphy. Above ~ 1050 m, thin shales and limestones appear, the dolomite darkens and the chert blackens. The upper Hüttenberg is recessive overall, but resistant layers of very coarse oolite occur in the Otavi Mountains (King, 1993). On the Fransfontein slope and Outjo basin, the upper Tsumeb is represented by allodapic dolostone and derived debris flows. The major change from peritidal to allodapic facies groups is cut out by sub-Mulden erosion south of Kamanjab (Fig. 2) but is constrained to occur in <10 km across strike (see Excursion Day 3). On the upper dip-slope of the Huab ridge (Fig. 3) on Heuwels farm, the basal (pink tepee) member of the Elandshoek Formation is in typical platformal facies. East and west of Fransfontein (Fig. 2), foreslope facies prevail except locally near the top of the preserved section, where high-energy shelf-break facies (coarse crossbedded oolite and large domal stromatolites) are encountered, reflecting minor progradation of the platform margin (Fig. 3).

Work remains to be done on the $\delta^{13}\text{C}$ profile of the upper Tsumeb. On the platform, the basal tepee member begins at -2 per mil, descends to -3 per mil, and then rises to -1 per mil (Fig. 18). The grainstone cycles that make up the bulk of the Elandshoek Formation hover around -1 per mil (Fig. 4). The lower Hüttenberg stromatolite (*tuten*) member is highly variable within a statistical envelope of 0 and 4 per mil. In the Otavi Mountains, the upper

Hüttenberg climbs to ~10 per mil before returning to 0 per mil at the top (Kaufman et al., 1991). A condensed but somewhat similar pattern is observed on the Fransfontein slope (Kennedy et al., 1998). Above the negative Maieberg anomaly, values first stabilize near 1 per mil (~2 per mil higher than on the platform), then become more variable between -1 and 3 per mil. Around 300 m up-section, they rise to 5 per mil before falling back near the top. At present, it is not known if the 5 per mil excursion on the slope is equivalent to the 10 per mil upper Hüttenberg excursion on the platform. If this were true, then the entire Tsumeb subgroup would be represented on the slope, but reduced to ~400 m in thickness compared with ~1900 m on the platform. Alternatively, the 5 per mil excursion on the slope might belong to the isotopically-unstable stromatolitic interval of the lower Hüttenberg on the platform.

Bruce Runnegar recently postulated (see also Fölling and Frimmel, 2002) that the 5 per mil upper Tsumeb slope excursion (Kennedy et al., 1998) is correlative with the 5 per mil excursion in the Zaris Formation (Kuibis subgroup) of the lower Nama Group in southern Namibia (Saylor et al., 1998), which is dated on its descending limb by a U-Pb zircon age from a tuff of 549 ± 1 Ma (Grotzinger, et al., 1995). Barring unexpected success in dating tuffs from the upper Otavi Group (where all previous attempts have failed for lack of primary zircons), independent support for the proposed upper Tsumeb-Kuibis correlation will likely depend on the calcified macrofossil assemblage *Cloudina-Namacalathus* (Grant, 1990; Grotzinger et al., 2000), which is characteristic of the lower Nama Group and Vendian carbonates of appropriate facies world-wide. To date, this fossil assemblage has not been found in the upper Tsumeb subgroup.

Mulden Group

A regional description of the Mulden Group is unnecessary here. We will drive through this clastic succession in the Achas syncline on Day 3 (Fig. 2). There the Mulden Group comprises three formations. At the base is a discontinuous and laterally variable unit of argillite, carbonate-clast fanglomerate, and argillite-hosted debris flows that onlaps a landscape-scale karst exposing the entire Otavi Group with local relief of >250 m (Frets, 1969). Germs (1995) suggested that the pre-Mulden sea-level fall was glacial in origin whereas Hoffman and Hartz (1999) hypothesized a Messinian-type draw down associated with ocean closure. The succeeding Tschudi Formation (SACS, 1980) is a thick blanket of reddish-brown, lithic sandstone with m-scale tabular crossbeds indicating strongly southeast-directed fluvial paleoflow. The overlying Owambo Formation (SACS, 1980) consists of fine-grained mixed clastics of marine or estuarine origin.

DISCUSSION

The Snowball Earth hypothesis (Kirschvink, 1992) was conceived to account for paleomagnetic evidence in the late Neoproterozoic for glaciation at sea level close to the equator (Embleton and Williams, 1986). The paleomagnetic evidence is now virtually unassailable (Schmidt et al., 1991; Schmidt and Williams, 1995; Sohl et al., 1999; Evans, 2000). Kirschvink (1992) also pointed out that a snowball ocean would be anoxic and hydrothermally-dominated, thus accounting for the unique occurrence of banded iron-formation with glaciomarine deposits in the late Neoproterozoic (see also Klein and Beukes, 1993; Canfield and Raiswell, 1999). He also predicted (Kirschvink, 1992) that snowball terminations should leave a global sedimentary record of abrupt climate change due to reverse ice-albedo feedback and the extreme greenhouse forcing required to overcome the snowball albedo (Caldeira and Kasting, 1992). Hoffman et al. (1998) argued that cap carbonates, long recognized as peculiar to the late Neoproterozoic (Kröner, 1977; Fairchild, 1995; Grotzinger and Knoll, 1995; Kennedy, 1996), are the predicted post-glacial deposits, with carbonate production driven by global warming and an alkalinity flux driven by intense carbonate and silicate weathering (see also Hoffman and Schrag, 2000; 2002). In addition, the abrupt onset of glaciation in Namibia and other low-paleolatitude regions is consistent with ice-albedo runaway. For the Ghaub glaciation, the absence of paleotopography on the Otavi platform rules out mountain glaciers, consistent with the preponderance of locally-sourced carbonate debris, and suggests that glacial transport may have been powered by “sea glaciers” (Warren et al., 2002). Finally, large carbon isotopic excursions in seawater proxies bracketing the glacial deposits (Kaufman et al., 1997; Hoffman et al., 1998; Halverson et al., 2002) can be quantitatively explained by the snowball hypothesis (Higgins, 2002; Schrag et al., 2002). Moreover, comprehensive geochemical modeling of seawater carbon and strontium isotopic response to the snowball cycle (Higgins, 2002) shows that criticisms of

the hypothesis on those grounds (Jacobsen and Kaufman, 1999; Kennedy et al., 2001a) are not valid. Still, extravagant claims must be supported by extraordinary facts. The stratigraphic setting of glacial deposits in the Otavi Group is extraordinary, not in comparison with other late Neoproterozoic successions, but by contrast with glaciation of any other Eon.

DAILY EXCURSION LOG

Day 1. Windhoek to Tweelingskop

Depart Hotel Safari (set trip odometer to 0.0 km) at 0730 hrs. At Hotel exit, turn left onto Aviation Road, then left again onto *Auas*. At the first traffic light (1.0 km), continue straight on the route now named Hosea Kutako. Follow *Hosea Kutako* northward to Independence (6.4 km). Turn left on *Independence* for 0.7 km to the B1 interchange (7.1 km). Turn right onto **B1** and proceed north for 71 km to *Okahandja* (78 km). The north-dipping strata are semi-pelitic schists of the Khomas accretionary prism. Follow B1 around Okahandja and continue northward for 173 km to *Otjiwarongo* (251 km). In Otjiwarongo, turn left at the central square onto *Dr Libertina Amathila* (C38). Proceed northwest on **C38** for 73 km to *Outjo* (324 km). We will refuel at the CalTex station in Outjo and order lunch to go at the bakery across the road. Just north of Outjo, turn left onto **C39** and proceed west for 132 km to *Khorixas* (456 km). The sealed road ends at Khorixas; reduce your speed on gravel and be alert for dust clouds from passing vehicles. Continue west on C39 for 40 km (496 km), then turn right onto a side road heading northwest with a hand-painted sign “Ersbegin Date Farm”. (If you reach the “Petrified Forest” [Cretaceous Etjo sandstone] kiosk, you have gone 5 km too far west on the main road.) Proceed northwest on the Date Farm side road for 40 km to the Huab River (536 km). Turn right and follow the river northeastward (do not enter the date farm) for 16 km (552 km). In daylight, you should be able recognize the koppie in Fig. 6 behind you on the right (looking south). We will camp on the right bank of the river overnight. Leave room for elephants to pass by in the night and do not stray far from camp.

Day 2. Ghaub glaciation on the Huab ridge

(Huab River at lat. 20°07'S, long. 14°35'E on Tweelingskop 676 farm)

Today we will climb through a section of carbonates bounding the Ghaub glaciation, located on the upper dip-slope of the Huab ridge (Fig. 3) near the edge of the Otavi platform. *The first part of the climb is steep in places, so please be aware at all times of persons directly above or below you, and try to avoid dislodging loose rock.* Consult Fig. 6 for a ground-level photograph of the ridge to be climbed and the stratigraphic units to be examined. A stratigraphic column with isotopic data and space for your notation is given in Fig. 7. After reaching the top of the ridge, we will traverse northeastwards along strike to see different aspects of the Maieberg cap-carbonate sequence. The route is indicated on the air photo (Fig. 5), which also shows the mapping by Gad Soffer (1998) that forms the basis for the stratigraphic cut-off relations in Fig. 3. Points of interest on the traverse are numbered in accord with the paragraph headings below. Unless you are fleet of foot, two days are required to visit all the numbered sites. For the IAS Excursion, we will traverse from site [2-1] to [2-10], time permitting. You must leave site [2-9] no later than 1615 hrs to have sufficient daylight to usefully visit site [2-10]. Otherwise, you should return to camp by the river directly from site [2-9]. If you have two full days to spend here, I recommend traversing sites [2-10] through [2-16] *in reverse order* on Day 1, and sites [2-1] through [2-9] on Day 2. *Beware of elephants in the river valley—they are not dangerous provided you keep your distance. Ears flapping is a sign of displeasure—cautiously retreat.*

[2-1] **Paleoproterozoic metamorphic complex.** The climb begins in sheared, K-feldspar±quartz-phyric, metavolcanic rocks dated elsewhere in the Kamanjab inlier at 1.98 Ga (unpublished zircon Pb-Pb age by Alfred Kröner). Metamorphism of the crystal tuffs(?) produced unoriented amphibole needles and retrograde biotite. The basement was metamorphosed twice, to amphibolite grade in the Paleoproterozoic (ca 1.95 Ga) and to greenschist grade in the Damaran orogeny (ca 550 Ma). The steep, southeast-dipping foliation in chloritic schist beneath the sub-Otavi unconformity is probably Damaran.

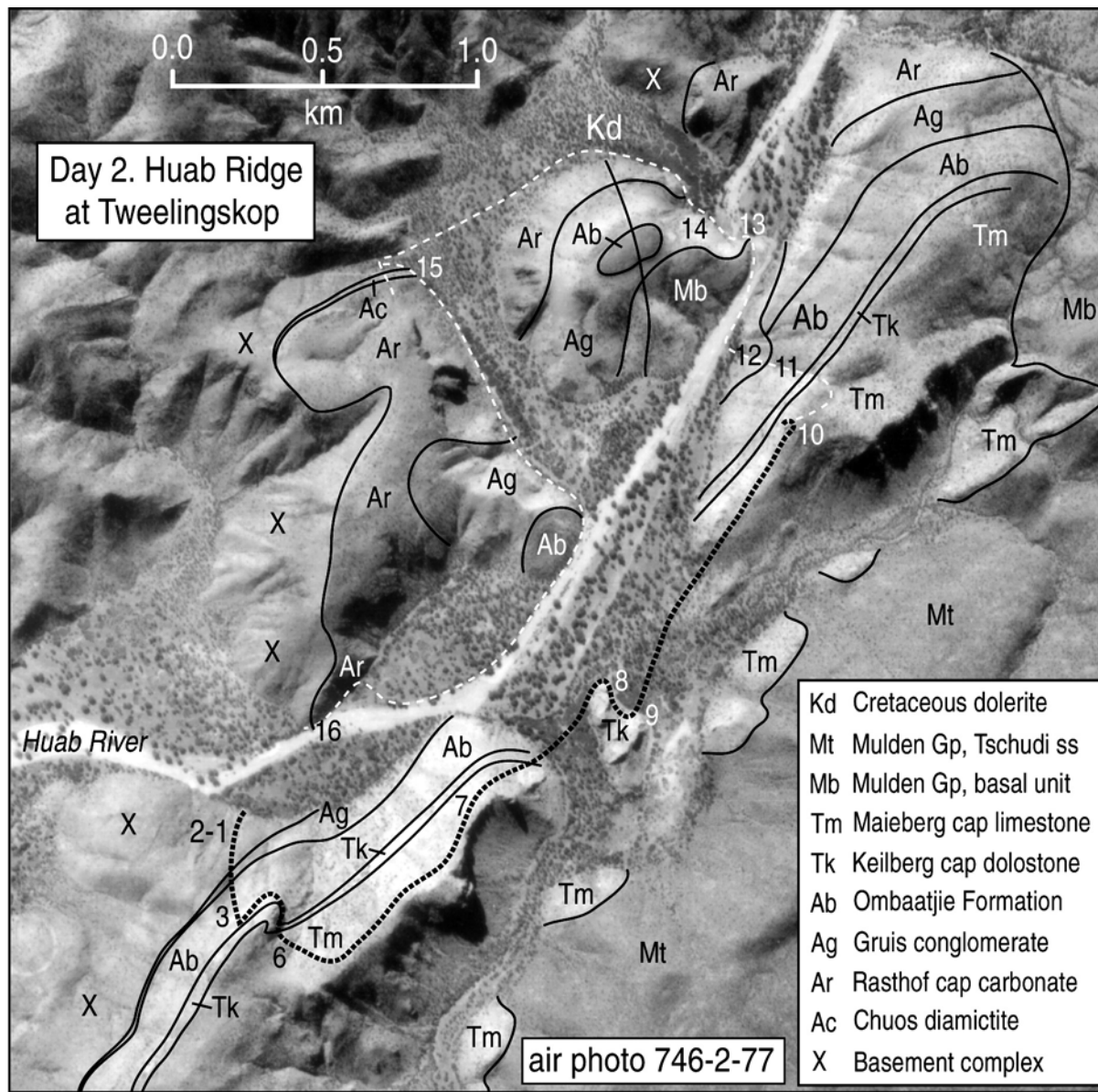


Fig. 5. Traverse photo map for Day 2. Black stippled line is the Excursion traverse with numbered stops. White dashed line is an alternative traverse. Geology modified from Soffer (1998).

[2-2] **Gruis Formation.** The Gruis Formation directly overlies the basement in this section; the southern limit of the Rasthof Formation is 0.5 km to the north (Fig. 5). The Gruis Formation totals 45 m thick, of which the lower 37 m consists of fanglomerate containing clasts of tonalitic orthogneiss and vein quartz. North of the section, scattered stromatolites composed of tan dolomite occur within the fanglomerate, which thickens rapidly in the same direction. Rasthof dolostone clasts are absent, which rules out paleoflow from the north given evidence elsewhere that dolostone clasts were easily eroded and transported in the arid or semi-arid Gruis-age climate. Pebble imbrication in conjunction with ripple crests and quaquaversal dips of crudely-stratified fanglomerate in other sections indicate paleoflow was directed northward, consistent with grain-size and lithofacies changes. The fanglomerate becomes finer-grained at the top and is overlain by 8 m of m-scale cycles in which conglomeratic sandstone with scoured bases are overlain by tan dolostone microbialaminite with tepee structures. The last pebbly bed is reverse-graded and uniquely rich in “smoky” quartz clasts. The top of the Gruis Formation is a ferruginous exposure surface atop 30 cm of tan dolostone microbialaminite with sandstone lenses and “floating” quartz pebbles.

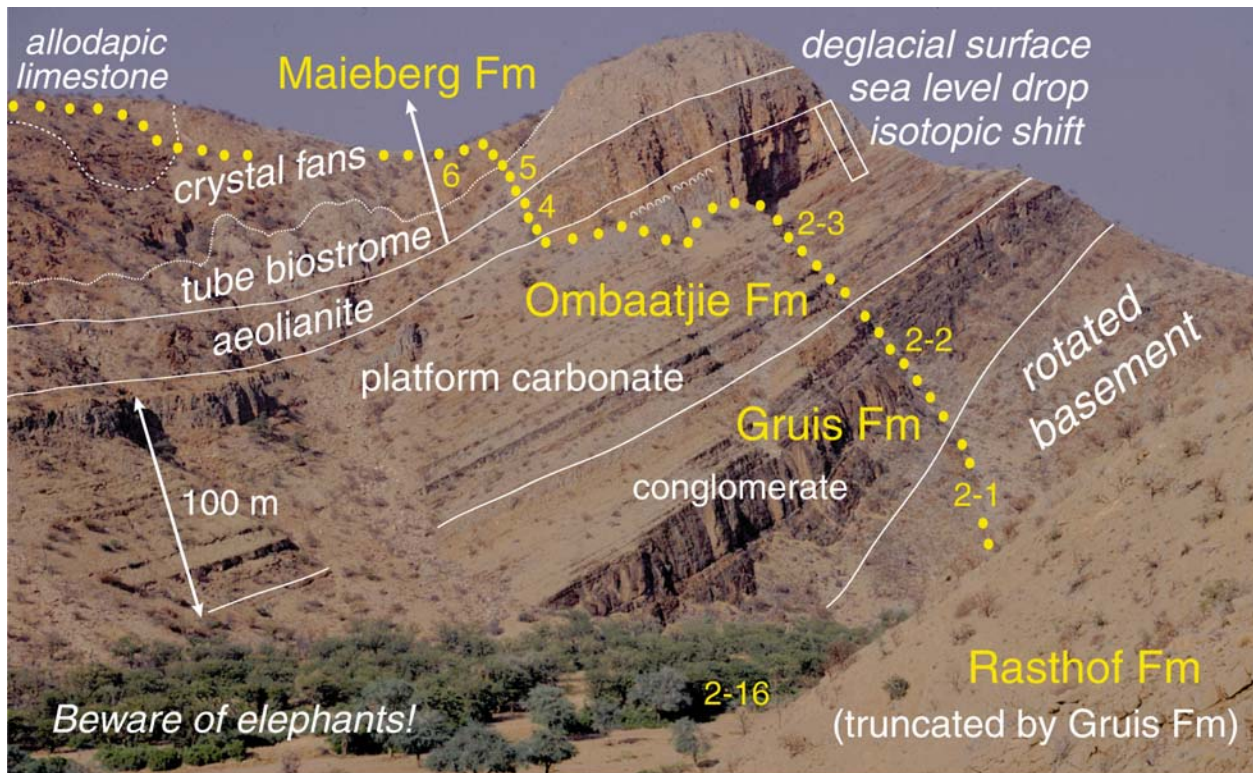


Fig. 6. Photographic guide for the morning traverse on Day 2, located on the Huab River near the western edge of the farm Tweelingskop 676 at latitude 20 deg. 07'S and longitude 14 deg. 35'E. Modified from Soffer (1998).

[2-3] **Ombaatjie Formation.** The Ombaatjie Formation is a retrogradational set of eight parasequences totalling 102 m thick in this section (Fig. 7). The first four parasequences are strongly condensed compared with sections on the Hoanib shelf, consisting of argillite capped by resistant beds of black limestone. The primary nature of the limestone is difficult to discern because of tectonic foliation and recrystallization, but my tentative interpretation is that they are composed of mounded thrombolites and intervening grainstone. The limestone-capped parasequences are separated by marine flooding surfaces with no evidence of exposure. Parasequence 5 is also shale-dominated but is capped by grey dolostone microbialaminite, as is parasequence 6 which is strongly condensed. It forms a steep little pitch leading to the shady overhang at the base of a rock wall we will not climb! Up to this point, $\delta^{13}\text{C}$ in this and correlative sections to the east hover near +5 per mil (Halverson et al., 2002). The pre-glacial decline in $\delta^{13}\text{C}$ of ~10 per mil occurs in parasequence 7 (Fig. 7), which is abnormally thick (37.6 m) in this section. We will first traverse along the base of the cliff towards the northeast and then angle up-section around the nose of the ridge, following the route marked on Fig. 6. Parasequence 7 begins with 5.5 m of argillite, exposed below the overhang, but it is dominated by light grey dolostone “ribbons” and thick-bedded cherty grainstone, with two thin bands of microbialaminite about half-way up. At the top of the parasequence is a well-developed *Tungussia*-type stromatolite, 3.5 m thick. Stromatolites are prominent at this horizon in all sections on the Huab ridge, locally forming large columns of *Conophyton*. A marine flooding surface (along strike a karstic surface) atop the stromatolite begins the final parasequence which consists of 6 m of brownish marly dolostone with hummocky cross-stratification, abruptly capped by 1 m of tannish grey dolostone microbialaminite with a brecciated exposure surface at the top. This signals the sea-level fall associated with the Ghaub glaciation.

Day 2. Tweelingskop, Huab ridge

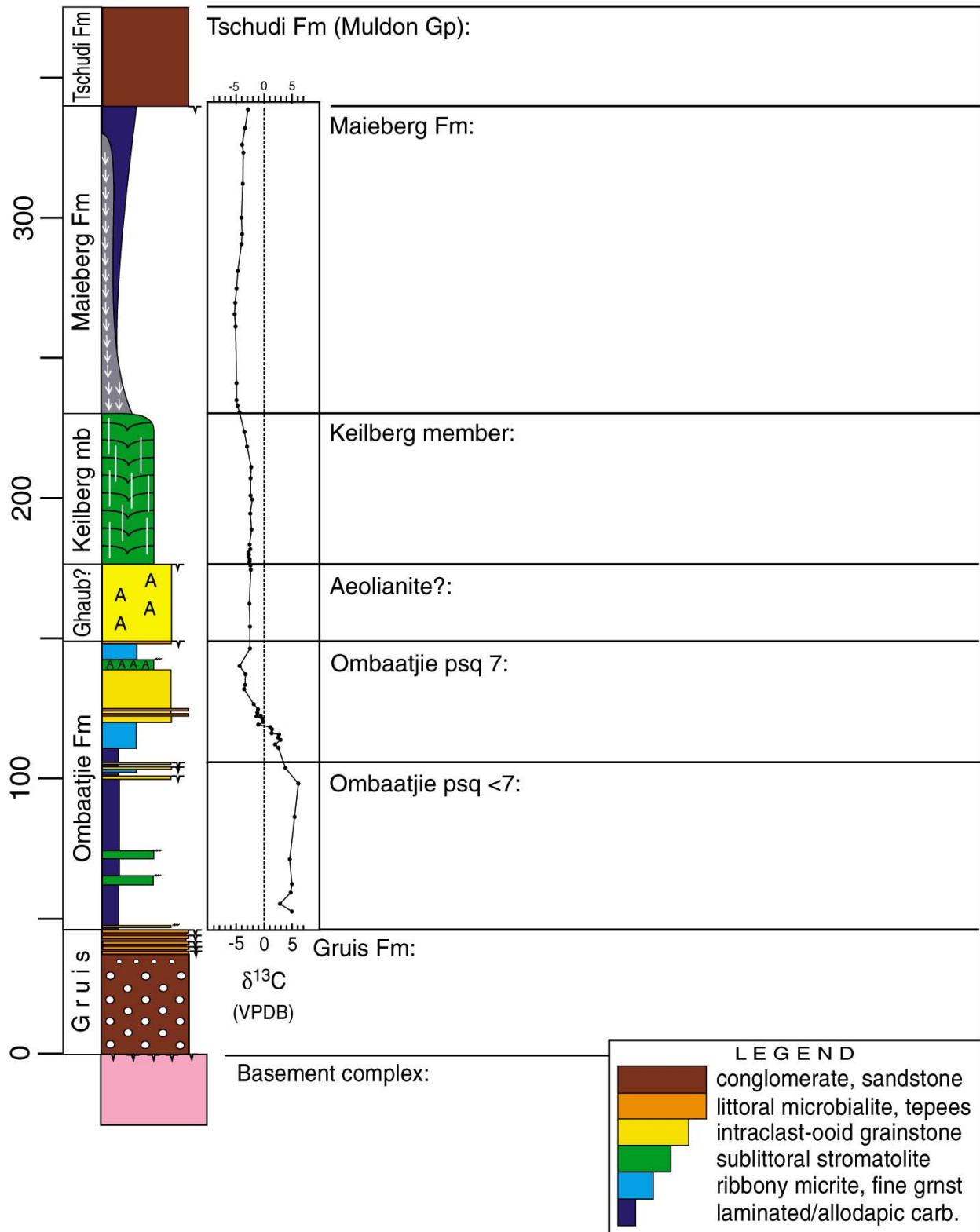


Fig. 7. Columnar section and carbon isotopic data for Day 2.

[2-4] **Ghaub(?) dolostone aeolianite.** The Ghaub diamictite is nowhere preserved on the Huab ridge. In its place

in this section is 28 m of massive, pervasively recrystallized, light grey dolostone (Fig. 7). This unit disappears rapidly northward and appears limited to the southernmost exposures of the Ombaatjie platform, those closest to the major regional shelf break (Fig. 3). The distribution and massive uniformity of this unit first aroused suspicion of an aeolian origin. During the 1999 annual field excursion, Sharad Master (Wits) identified typical aeolian “pinstripe” lamination. Large-scale foreset bedding near the top is oriented consistent with onshore transport (paleowinds from the south-southeast). Accepting the aeolian interpretation, the most reasonable inference is that it represents a cold-desert dune field developed at the windward edge of the platform following the sea-level fall associated with the Ghaub glaciation. Secondary silicification increases towards the top of the unit, which is brecciated. The top of the unit is a smooth sharp surface overlain by the distinctly paler Keilberg cap dolostone (Fig. 6).

[2-5] **Keilberg cap dolostone.** The Keilberg section is typical for the Huab (or Makalani) ridge. It is ~55 m thick but this is quite variable due to large-scale stromatolitic undulations (Fig. 6). It consists of dense, very pale, lightly-silicified dolostone. The basal meter is laminated abiotically, as is the top 10 m, but the rest of the unit consists of contiguous, m-scale, domal to corrugate stromatolites with indistinct lamination on account of lithologic uniformity. Preferentially silicified tubular structures invariably stand paleovertical within the stromatolites, irrespective of the primary dip of the stromatolitic lamination. The vertical orientation supports an origin by fluid or gas escape. As the structures do not occur at the base of the unit, the fluid or gas must have been generated within the cap dolostone, rather than from the underlying aeolianite as in the permafrost-methane hypothesis (Kennedy et al., 2001). During the 1999 annual field excursion, Dan Schrag (Harvard) postulated that the tubes originate from CO₂ escape, driven by rapid precipitation of carbonate from critically oversaturated pore water. Unfortunately, lithologic homogeneity, recrystallization and silicification conspire to obscure the true nature of the tubular structures in this facies. Presumed analogous, but much better preserved, tubular structures will be seen on the Hoanib shelf on Excursion Day 6.

[2-6] **“Crystal Palace” in the Maieberg cap-carbonate sequence.** A marine flooding surface separates the Keilberg dolostone from the deeper-water limestones and cherty dolomites of the middle Maieberg. Normally, this interval consists of pinkish allodapic and micritic limestone, or rhythmically alternating limestone, dolostone and marl. In this section, the normal sediment is augmented and baffled by profligate sea-floor cement. The cement, which is most visible where partially dolomitized or silicified, basically consists of cm-scale sheaves, or “pin-cushions”, of needle-like prismatic crystal pseudomorphs, mostly now composed of void-filling spar. The squared-off tips and notched, pseudo-hexagonal cross-sections of the mm-scale pseudomorphs are readily apparent in thin section, and locally in outcrop, leaving no doubt that the primary cement phase was aragonite (orthorhombic CaCO₃). Over time, the crystal pin-cushions evolved to form m-scale arborescent “thickets” in vertical section, although they never actually projected far above the surrounding sediment surface. At the decameter scale, reef-like masses dominated by cement apparently did project several meters above the adjacent, allodapic-dominated depressions (Fig. 6). The thickness of the cement-rich interval is ~100 m, nearly half the Maieberg cap-carbonate sequence above the Keilberg cap dolostone. The cements resemble those commonly found in Archean and Paleoproterozoic carbonates (Grotzinger and Knoll, 1995) except that the older cementstones lack associated micrite (Sumner, in press), which did “rain” down upon the Maieberg cements. In this, as well as in overall extravagance, stratigraphic position and paleogeographic location, the Maieberg cements are closely similar to those in presumed correlative cap carbonates elsewhere (Grotzinger and James, 2000). Only in cap carbonates are cements of this nature found in the Neoproterozoic, and they imply that bottom waters 10s of metres deep were critically oversaturated at the platform margin during the maximum post-glacial flooding stage. A somewhat different form

of cement will be seen in the “Rose Garden” at location [2-10]. To get there, it is best to traverse northeastward on the crest of the ridge (Fig. 5).

[2-7] **Silicified crystal fans.** There is a photogenic wall of selectively silicified crystal fans near the end of the ridge, just below the ridge-crest on the northwest side. From here, proceed to the end of the ridge and then carefully descend, heading toward the prominent white outcrops of Keilberg dolostone that stick up above the trees on the valley floor at locations [2-8] and [2-9].

[2-8] **Silicified void-filling crystal fans in the Keilberg cap dolostone.** This outcrop appears to be near the base of the Keilberg cap dolostone. The dolostone is brecciated and hosts m-scale, void-filling, crystal fans of presumed former aragonite replaced by dolomite or silica. They are most visible where they are silicified. The void-filling habit of the Keilberg crystal fans is distinct from the sea-floor cements in the overlying Maieberg sequence.

[2-9] **Mega-stromatolites and vertical tubular structures in the Keilberg dolostone.** This is a fair outcrop to examine the large-scale stromatolites of which the Keilberg in this facies is predominantly composed. The individual “stromatoids” are defined by laminae that have broad central arches but steeply draped flanks. Selectively silicified tubular structures ca 2 cm in diameter occur in both the central and peripheral parts of the contiguous stromatoids and invariably paleo-vertical irrespective of the dip of the stromatolitic lamination. Time permitting, proceed northeastward parallel to the river toward the end of the next on-strike ridge. Ascend the crest of the ridge to location [2-10].

[2-10] **“Rose Garden” in the Maieberg cap-carbonate sequence.** Here we see a somewhat different, visually attractive style of pseudomorphosed aragonite cement formed on the sea floor. The cement takes the form of m-scale sheaves, or “bouquets”, of recrystallized pink limestone that contrast with the tanish grey colour of the allodapic host limestone. Relations between the allodapic layers and cement indicates that the latter projected up to several centimeters above the sea floor but were episodically annihilated through sediment burial. In similar facies of the less metamorphosed Ice Brook cap carbonate in Canada, the $\delta^{18}\text{O}$ of the cements (no void-filling spar) is significantly higher by up to 4 per mil compared with coeval allodapic micrite. Assuming primary aragonite for both, the difference implies a contrast in temperature and salinity between the bottom waters from which the cement precipitated and the surface waters that produced the allodapic sediment. Given sufficient water depth, this is not unreasonable in the aftermath of a snowball episode, when cold saline bottom water from beneath a global ice shell was flooded by meltwater strongly warmed by greenhouse forcing. An unusually stable density stratification would result. Nevertheless, the oceanic overturning circulation would eventually resume due to diffusive dissipation of the salinity-induced density gradient. The localization at major shelf breaks of sea-floor cements in cap-carbonate

sequences suggests an upwelling source of alkalinity in addition that that provided to the surface ocean by carbonate weathering and runoff.

[2-11] **Upper Ombaatjie Formation.** This section is similar to that at [2-3] except that a karstic surface with >3 m local relief is developed upon the stromatolite bed at the top of parasequence 7, and the lower third of the formation is covered.

[2-12] **Mulden Group talus breccia and Keilberg “tube” puzzle.** The lower part of the gully exposes a spectacular carbonate-clast conglomerate and mega-breccia with a greenish siltstone matrix. It belongs to the lower Mulden Group sedimentary assemblage that fills mega-karstic paleovalleys, under re-excavation by the modern Huab River drainage system. Mulden-age colluvial deposits “plaster” many of the modern valley walls. At this location, the carbonate debris is hosted by subaqueously deposited siltstone, implying that the paleovalleys contained lakes or estuaries. Large blocks of Keilberg cap dolostone are particularly prominent and permit close examination of their enigmatic tubular structures. An adjacent pair of half-meter sized blocks with tubes oriented parallel and normal to the outcrop surface, respectively, are particularly noteworthy. In each block, the tubes are filled partly by brownish dolomicrite and partly by white calcite spar, consistent with an origin by gas escape. Accordingly, the tubes were oriented subvertically when they formed. Now, here is a puzzle for you to solve. Why is the host lamination steeply inclined with respect to the outcrop surface in both blocks? What is the angular relation between the lamination and the tubes in each block? What does this tell you about the shape of the lamination? Your examination of site [2-9] should help you solve the puzzle.

[2-13] **Mulden Group “buttress” unconformity.** This is a fine example of a “buttress” unconformity, or high-angle onlap, of basal Mulden Group deposits against a truncated syncline of Gruis Formation impure dolostone.

[2-14] **Gruis Formation.** Although this section is only 2 km north of [2-2], it is obviously more distal lithologically. It is dominantly composed of m-scale parasequences dominated by tan dolostone microbalaminite. Terrigenous clastics are subordinate and distinctly finer than to the south. Correlations suggest that the basal fanglomerate at [2-2] is not basal with respect to sections to the north.

[2-15] **Chuos diamictite.** This is the only significant section of Chuos diamictite on the Huab ridge. It rests sharply on a smoothed erosion surface developed on retrograded granodiorite. The Chuos consists of up to 36 m of massive to very poorly stratified diamictite, composed of rounded boulders and stones of basement material in a non-sorted wackestone matrix. The Chuos-Rasthof contact is highly unusual. It is transitional, but this appears to be due to slope instability and remobilization of the diamicton after Rasthof cap-carbonate deposition had begun. The primary diamictite is overlain by 12 m of roundstone paraconglomerate with rare dolostone clasts and silt lenses. This is followed by over 50 m of argillite choked with channelized, tan dolostone, debris flows. Distinctive Rasthof-type stromatolites can be seen in the debris. The debris flow direction has not been determined, but the Huab dip-slope could have been critically over-steepened during the Chuos glaciation if it was tectonically active at that time.

[2-16] **Rasthof cap dolostone.** The Chuos diamictite is missing here and the Rasthof cap dolostone rests directly on basement orthogneiss. To the south, within the valley, the Rasthof disappears beneath the Gruis Formation (Fig. 5). The basal Rasthof begins with 5 m of crudely stratified, finding-upward, dolostone breccia. The rest of the section consists of laminated and allodapic grey dolostone. Up to 280 m of Rasthof dolostone appear beneath the Gruis Formation north of the basal cut-off.

Day 3. Ghaub glaciation on the Fransfontein slope

(Lat. 20°11.443'S, long. 14°51.048'E near Narachaamspos)

After breaking camp early, we will drive back south down the Huab River and then ascend a major tributary from the east, the Soutrivier, that climbs through the Mulden Group into the axis of the Achas syncline. We will then drive eastward on a rough track in the axis of the syncline for ~25 km to the village Narachaamspos (Fig. 8). The total drive will take at least four hours. The section at Narachaamspos is among the most proximal on the Fransfontein slope (Fig. 3). We will not have time to traverse the Rasthof or Gruis in this section, each of which are >300 m thick. The Rasthof is a stack of debris flows composed of light-grey dolostone grainstone, stromatolite and isopachous cementstone. The Gruis consists mainly of green argillite with mixed quartz-dolomite turbidites and debris flows. We will leave the vehicles at the river crossing opposite the western terminus of the Otavi Group hills (Fig. 8) and follow a trail parallel to the river on the north side. We will then ascend a small tributary that re-excavates a paleovalley lined by basal Mulden alluvium, which is cleaved so as not to be confused with the

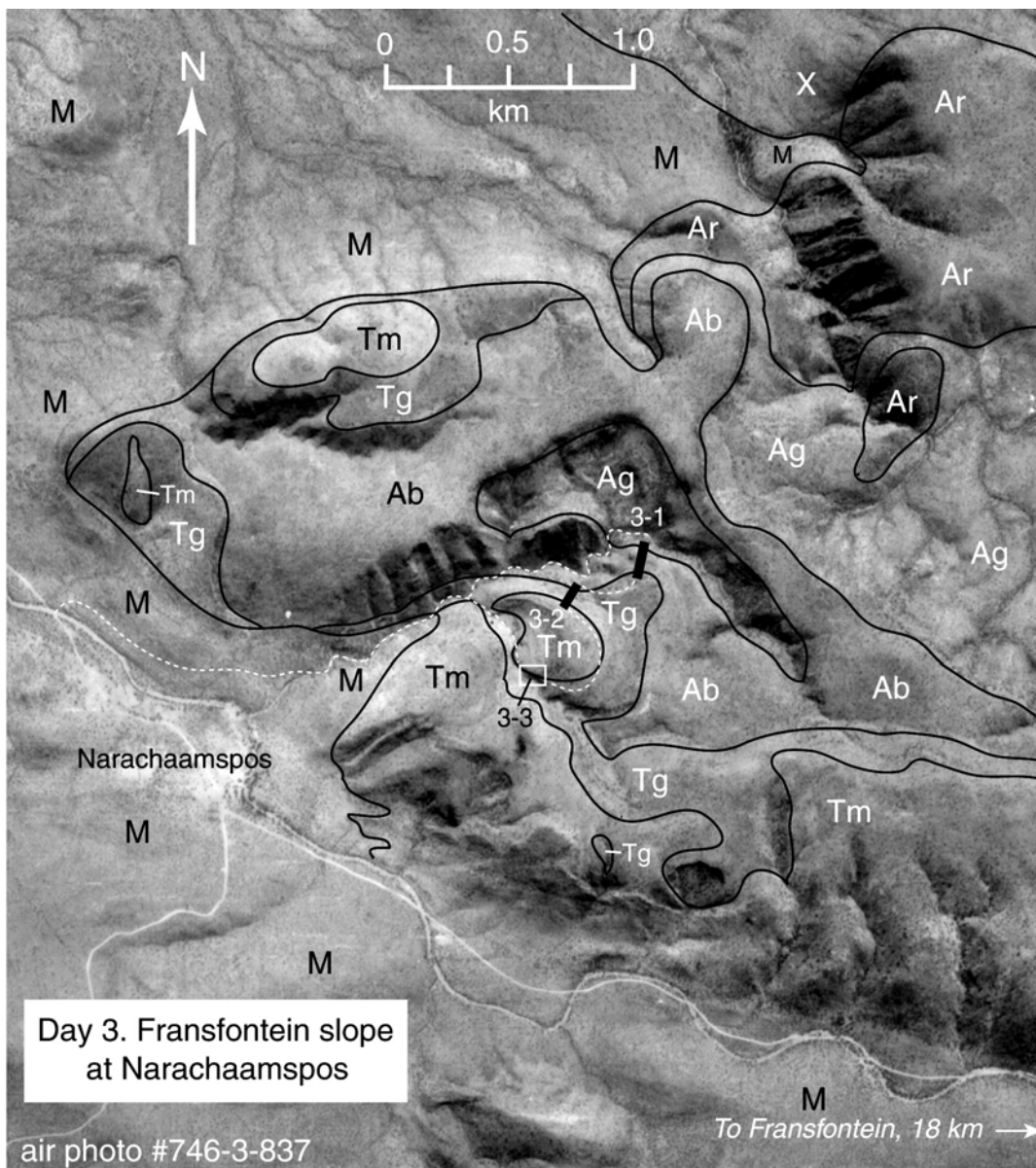


Fig. 8. Photo map for Day 3 traverse to section on the Fransfontein slope. The Otavi Group forms a paleokarstic ridge beneath the Mulden Group foreland basin clastics. Road is the white line following the river south of the Otavi ridge. Geology by D.C. Frets, P.F. Hoffman, G.P. Halverson and C. Carman.

Quaternary calcrete. Time permitting, we will follow the main channel to the base of the “Ombaatjie” Formation. We will then traverse southward across an 82-m “Ombaatjie” section [3-1], a 54-m section of Ghaub diamictite [3-2], and a classic exposure (Fig. 9) of the Ghaub-Maieberg contact at site [3-3] that is highly representative of the glacial termination throughout the Fransfontein slope. A composite columnar section with isotopic data is given in Fig. 10.

[3-1] **Pre-glacial “Ombaatjie” slope deposits.** The upper dolostone unit of the Abenab subgroup begins sharply on the less resistant, mixed clastic-carbonate turbidites of the Gruis Formation. The light-grey “Ombaatjie” dolostone consists essentially of three coarsening-upward cycles bounded by flooding surfaces. All begin with ribbony dololite that grades upward into sand or granule-sized grain-flows. Crossbedding is observed at the top of the first cycle. The third cycle is over half the total thickness and contains resedimented oolite, pisolite and isopachous cement. The detailed internal stratigraphy of this and other units on the slope is highly variable along strike, but their overall sedimentary character changes little. The isotopic characteristics and problems of correlation of this unit were discussed in the last paragraph under the heading *Upper Abenab subgroup* in the *Geological overview*. The top of the dolostone is a brecciated and silicified sequence boundary forming a topographic dip slope. Note the recessive green siltstone resting on the flooding surface and then angle down to the right into the drainage to the base of the Ghaub section at [3-2].



Fig. 9. Transition from Ghaub diamictite to Maieberg cap carbonate on the Fransfontein slope at Stop 3-3. Note the 2-m blanket of bedded diamictite with dropstones at the top of the Ghaub Fm, and the knife-sharp contact with the overlying, dropstone-free, cap dolostone. Galen P. Halverson for scale.

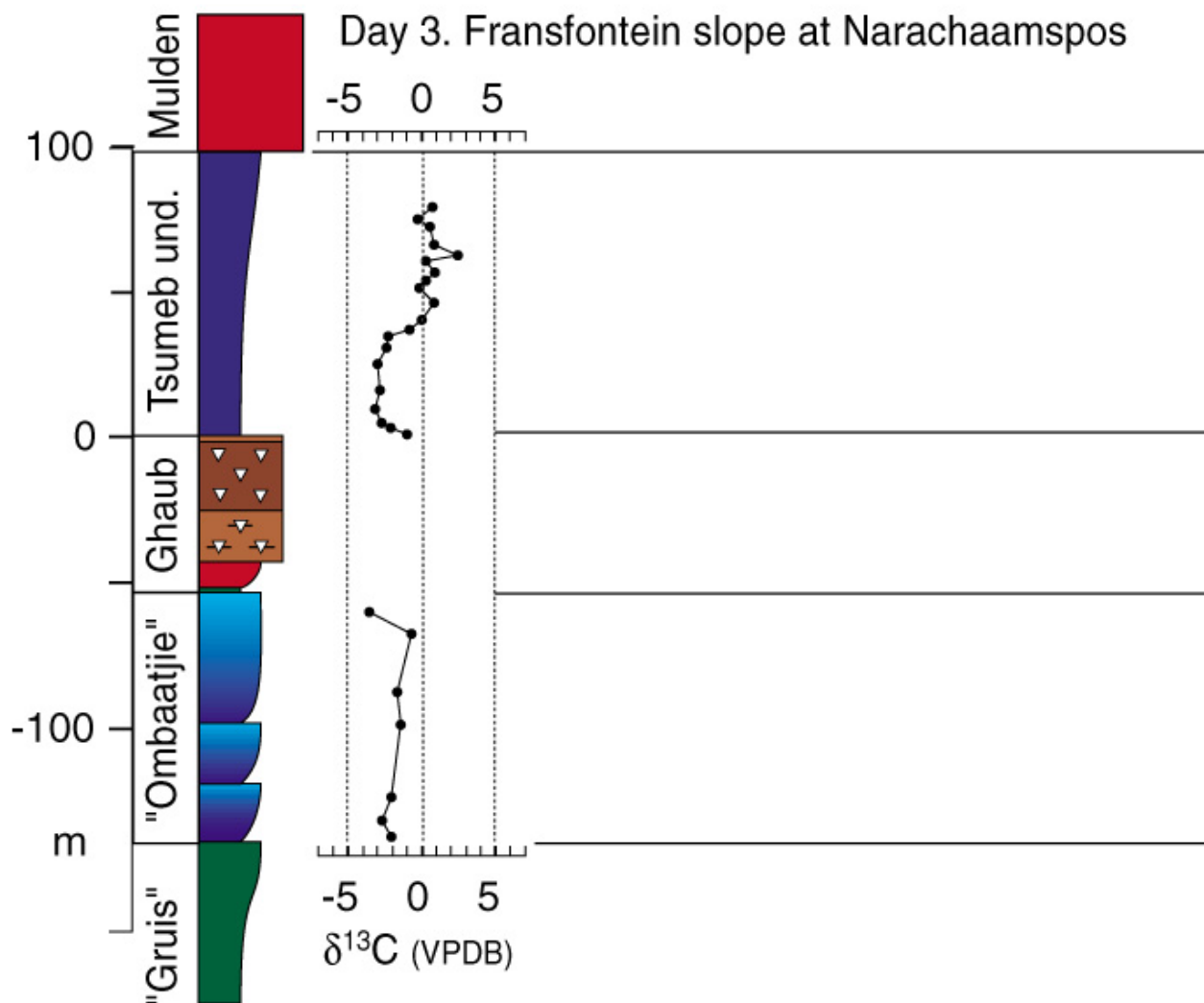


Fig. 10. Columnar section and carbon isotopic data for Day 3.

[3-2] **Ghaub diamictite.** The section begins with 10 m of siltstone (loess?) and sandstone of mixed provenance. This ends at a submarine(?) erosion surface overlain by 15 m of stratified carbonate diamictite inter-layered with mixed (quartz-dolomite) sandstone and ribbony dololomite. The clasts in the diamictite include dolomite, limestone, pisolite, quartz and chert. Some of the sandstones have textural characteristics of aeolian ancestry. A ridge-forming unit of poorly-stratified diamictite 27 m thick forms the backbone of the unit. It contains thin and discontinuous sandstone interbeds and graded flow-units can be seen near the top of the diamictite. Clasts of pisolitic and stromatolitic dolostone are prominent, as are clasts of isopachous marine(?) cements similar to void-fillings in debris flows of the upper Rasthof Formation on the Huab ridge. These clasts are easily observed on the route to site [3-3]. The diamictite ends with a continuous ~2-m blanket of thin-bedded allodapic dolostone crowded with dropstones.

[3-3] **Ghaub-Maieberg contact.** This superb exposure and elegant setting should be left unaltered—no hammering please. At the foot of the section (Fig. 9) are three graded beds of resedimented diamictite. They end the ridge-forming diamictite interval at section [3-2]. The last graded bed is followed by a recessive layer of ashy claystone <10 cm thick. It contains no primary zircons. The widespread terminal Ghaub unit of bedded allodapic dolostone

with dropstones is 2 m thick. Dropstones up to a meter in size occur throughout this unit. It is overlain with an abrupt depositional contact by fine-grained, thin-bedded, allodapic dolostone (slightly marly at the base) of the basal Maieberg Formation in which outsize clasts are virtually absent. The contact shows no evidence for exposure, reworking or significant hiatus. The Ghaub glaciation, like the Chuos (see Excursion Day 5), terminated abruptly. Low-angle hummocky cross-lamination, ubiquitous in the basal Keilberg cap dolostone on the platform, is rare or absent here. There are no stromatolites nor the tubular structures they contain. Close to the base of the Maieberg is a laterally-continuous zone about 1 m thick in which the layering is undulatory (somewhat amplified tectonically) and riddled by paleohorizontal sheet cracks filled by radiaxial isopachous cement, now variably dolomite or chert. The cements appear to have formed penecontemporaneously on the sea floor, implying that slope-depth bottom waters were critically oversaturated at least temporarily. Above the cement-rich zone, ~100 m of allodapic dolostone is preserved beneath the sub-Mulden erosion surface in this section (Fig. 10). The negative post-glacial $\delta^{13}\text{C}$ excursion that encompasses 300-400 m of section on the platform occupies just 40 m in this section on the Fransfontein slope. Not later than 1700 hrs, depart the section heading down the drainage to the main tributary, whereupon retrace the route to the vehicles.

To reach the campsite, we will turn around and drive back along the road in a northwesterly direction for 0.5 km, then take the lesser-used fork to the right. Continue northward (towards Olifantswater) on this track for 3.5 km, where we will camp in a small clearing to the right of the track.

Day 4. Fransfontein slope to Hoanib shelf

Today we will drive 160 km as the crow flies across the depositional strike to the Hoanib shelf (Fig. 2). Not being crows, it will take us most of the day. We will first retrace our drive of last evening, continuing eastward through *Narachaamspos* (do not take the right fork past the village that heads south up the ridge). Drive eastward for **18 km** to *Fransfontein* (18.0 km), keeping the Otavi Group carbonate ridge to your left. Upon reaching the main north-south gravel road (**C35**) at *Fransfontein*, turn left and head north for **83 km** to *Kamanjab* (101.0 km) Immediately north of *Fransfontein*, the road descends stratigraphically through the Otavi Group, including a section of Ghaub diamictite 130 m thick that is well-exposed on the east side of the road.

At *Kamanjab*, turn left at the main intersection (C40) and stop at the Shell station for fuel, water and sundries. Then return to the main intersection, turn left and head north again on **C35** for **53.5 km** to the gated track (**3223**) entering *Marienhöhe* farm (154.5 km). Take the track through the gate and head west for **16.5 km** to the Veterinary Control gate (171.0 km), where you will be required to sign the log book before entering the Kaokoland open-range area. Taking the right fork beyond the gate, continue northwestward on a rough track for **27 km** to *Ombaatjie* (198.0 km), where the upper Hoanib River enters the Otavi Group karst mountains. Do not follow the river into the range (Fig. 17), but head northward on a rough track along the foot of the carbonate range, for **19.0 km** to Devede (217.0). Continue northward beyond Devede for **2.2 km** (219.2 km), then turn westward on a near-invisible track heading for the gap in the front range about 1.4 km away (see Fig. 11). Find the track on the right (north) side of the gap and follow it to a river crossing **2.3 km** (221.5 km) west from where we left the well-used track. Here we will camp overnight.

Day 5. Chuos glaciation on the Hoanib shelf

(Lat. 19° 07.35'S, long. 13° 56.1'E near Omutirapo)

Today we will examine the Chuos diamictite and its bounding carbonates near the abandoned village of Omutirapo on the Hoanib shelf. The section is in a natural amphitheatre 5 km long by 2 km wide within the frontal range of the Otavi fold belt (Fig. 11). Perhaps it is an exhumed Carboniferous glacial cirque, given that the main north-south valley between the Otavi range and the basement inlier is clearly of glacial origin (Martin, 1965)—note the *roche moutonnée* of Nosib sandstone in the lower right corner of Fig. 11. We will traverse to the south end of the amphitheatre (Fig. 11). Our section will begin in shallow-water carbonates of the middle Ombombo subgroup, from

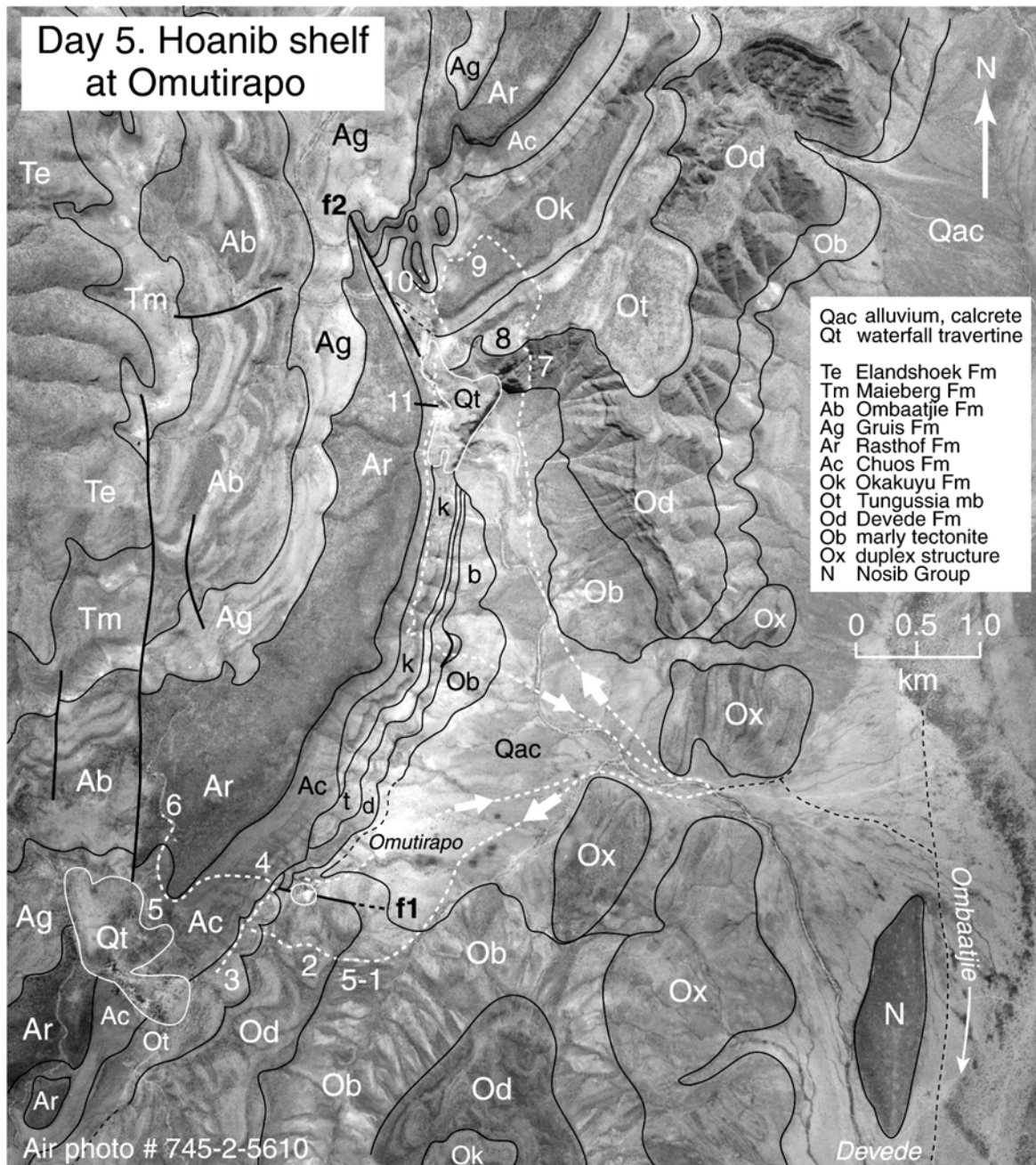


Fig. 11. Photo map for Day 5 traverse in the Omutirapo amphitheatre. Southern traverse (stops 5-1 to -6 is for the Excursion. The optional northern traverse (stops 7 through 11) is also described in the text. The two growth faults (f1 and f2) are indicated. Geology by P.F. Hoffman.

where we will first view and then climb a 450 m thick section of Chuos diamictite that abuts a paleoscarp formed of upper Ombombo strata with 385 m of local relief. At the top of the diamictite section, we will examine the basal contact and lower part of the Rasthof cap-carbonate sequence. We will return to camp no later than 1500 hrs, leaving time to drive back south to Ombaatjie with a stop en route at a section of middle and upper Rasthof Formation with excellent “roll-up” structures in sublittoral microbialaminite. An alternative full-day traverse to the north end of the Omutirapo amphitheatre is also indicated (Fig. 11) and briefly described.

First, a few words about the local structural geology. To first order, the structure is simply a gentle, west-dipping monocline. However, dolomites of the lower Ombombo subgroup (“Beesvlaakte Formation”) dip steeply to the east or west, discordant with the uniformly gentle (20-30°) westerly dips of the strata above and below. This dolomite (unit Ox in Fig. 11) is bounded above by argillaceous limestone tectonite (Ob) with an east-west stretching lineation and below by strongly cleaved argillite. Clearly, the steeply-dipping Ox dolomite occupies a duplex structure implying that the overlying strata could be horizontally displaced with respect to the autochthon. The second structural complication takes the form of relatively high-angle faults that were active at various times during Otavi Group deposition. Two such faults (f1 and f2 in Fig. 11) occur at either end of the amphitheatre. Both were active after Od and before Ot deposition, forming a horst between them (Fig. 12A). Fault f2 was inverted during and after Rasthof sedimentation, before the Gruis was deposited (Fig. 12B). The paleoscarp against which the Chuos diamictite was deposited (Fig. 13) could be localized by the f1 fault. It is not known if significant horizontal components of slip occurred on either fault. Groundwater seeps and resultant travertine deposits are strongly localized by these and other faults in the area.

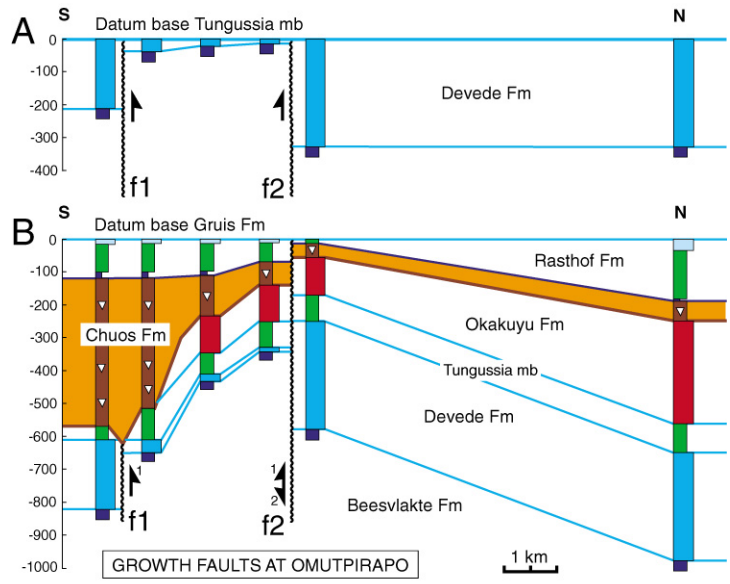


Fig. 12. Growth faults in the Omutirapo amphitheatre. Both faults were active after the Devede Fm and before the ‘pink Tungussia’ member (panel A). Fault ‘f2’ was inverted during Rasthof time. Faults dips and slip vectors are unknown and the fault traces are covered by Quaternary spring travertine.

[5-1] **Beesvlaakte tectonite.** The lower Ombombo duplex structure is accommodated by a roof detachment developed in recessive argillaceous limestone (unit Ob, Fig. 11). The resulting tectonite locally displays an east-west stretching lineation. The lack of “top” indicators in Ox dolostones thwarts structural resolution of the duplex structure—it could be contractional or extensional (Hoffman and Hartz, 1999) in origin.

[5-2] **Devede Fm mixed parasequences.** The middle Ombombo subgroup (unit Od) consists of up to 300 m of microbialaminite- or grainstone-capped parasequences composed of cherty, varicoloured dolostone and, in the lower part, alluvial conglomerate and sandstone. The clastics resulted from cannibalistic erosion of cover and basement on the Makalani dip slope (Fig. 3). Looking northwest from the crest of the ridge we see a panorama of the sub-Chuos paleoscarp (Fig. 13).

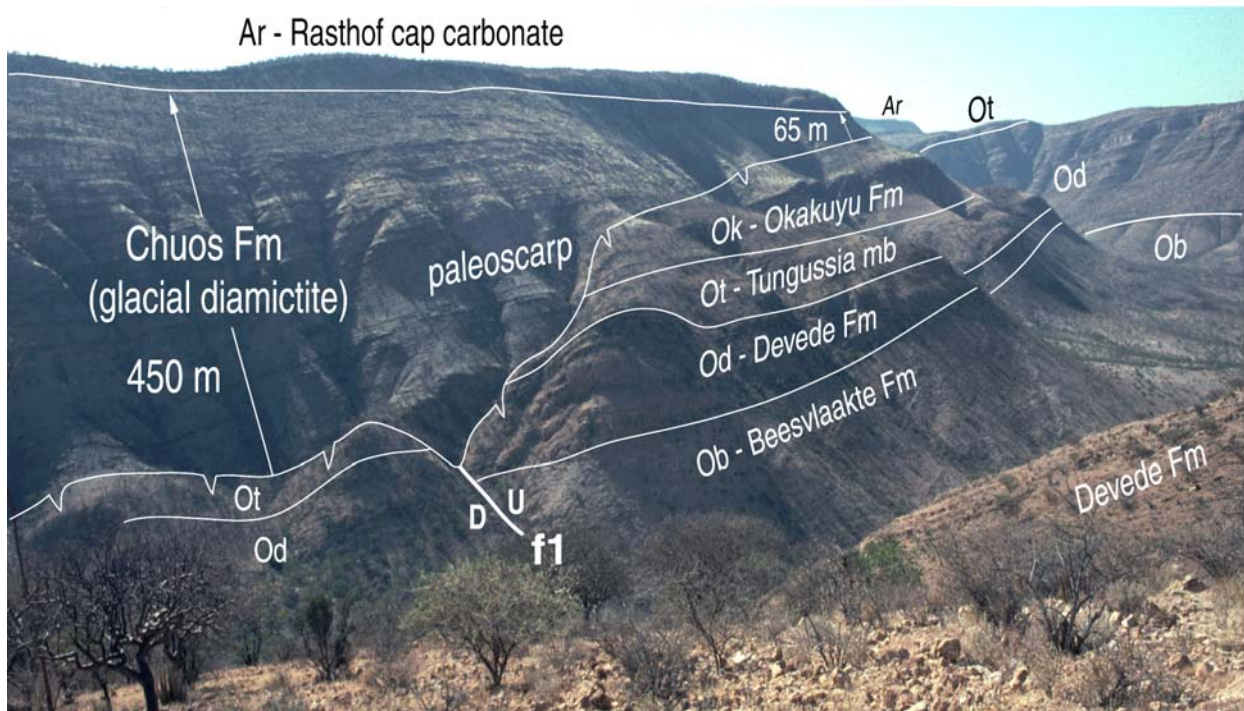


Fig. 13. View of the sub-Chuoss paleoscarp with ~385 m of local relief, looking northward from Stop 5-2 .

[5-3] **‘Pink Tungussia’ stromatolite member.** The middle Ombombo subgroup has a vertical component offset of 180 m, south side down, on the f2 fault (Fig. 12). Fault movement occurred prior to deposition of the “pink *Tungussia*” stromatolite member (unit Ot) at the base of the upper Ombombo subgroup, which projects across the fault line without significant vertical displacement. The stromatolite member is ~33 m thick in this section but the characteristic strongly-divergent branching habit is difficult to see on most surfaces because the lamination is faint. To the north, the stromatolite ends at a marine flooding surface overlain by <50 m of deeper water allodapic dolostone and maroon argillite. A sharp (erosive?) contact separates these beds from the retrogradational stack of coarsening-upward parasequences (Okakuyu Formation) composed of reddish-brown sandstone and conglomerate of southerly derivation.

[5-4] **Chuoss diamictite.** The Chuoss Formation is unusually thick, ~450 m, in this section. This is apparently related to the sub-Chuoss paleoscarp and a paleovalley at the foot of the scarp that may have been influenced by groundwater sapping from the f1 fault, despite there being no evidence of fault movement in Chuoss time. Over two-thirds of the Chuoss Formation consists of massive or sheared diamictite, composed of basement and cover debris in variable proportions. The diamictite is variably black, green, reddish-brown, or tan in colour. A thin unit of laminated siltstone with rare but excellent dropstones is discontinuously exposed at the base of the diamictite. Locally, large plate-like masses of the underlying dolostone were lifted or dislodged slightly, and the resultant voids are filled by fine diamictite. Similar structures are observed at the base of the Ghaub diamictite on the platform. The proposed explanation is that sea ice froze hard to the bottom but underwent surface ablation, resulting in positive buoyancy. The process would be most effective if the ice was thick, and could operate repetitively. Less than 20% of the formation consists of sandstone and conglomerate, locally with cross-beds indicating westerly

paleoflow, and there is a 50 m interval of green siltstone a little over half-way up section. The upper part of the formation is not well exposed but the few outcrops are diamictite. There is no evidence of subaerial exposure and the diamictite is presumably glaciomarine in origin.

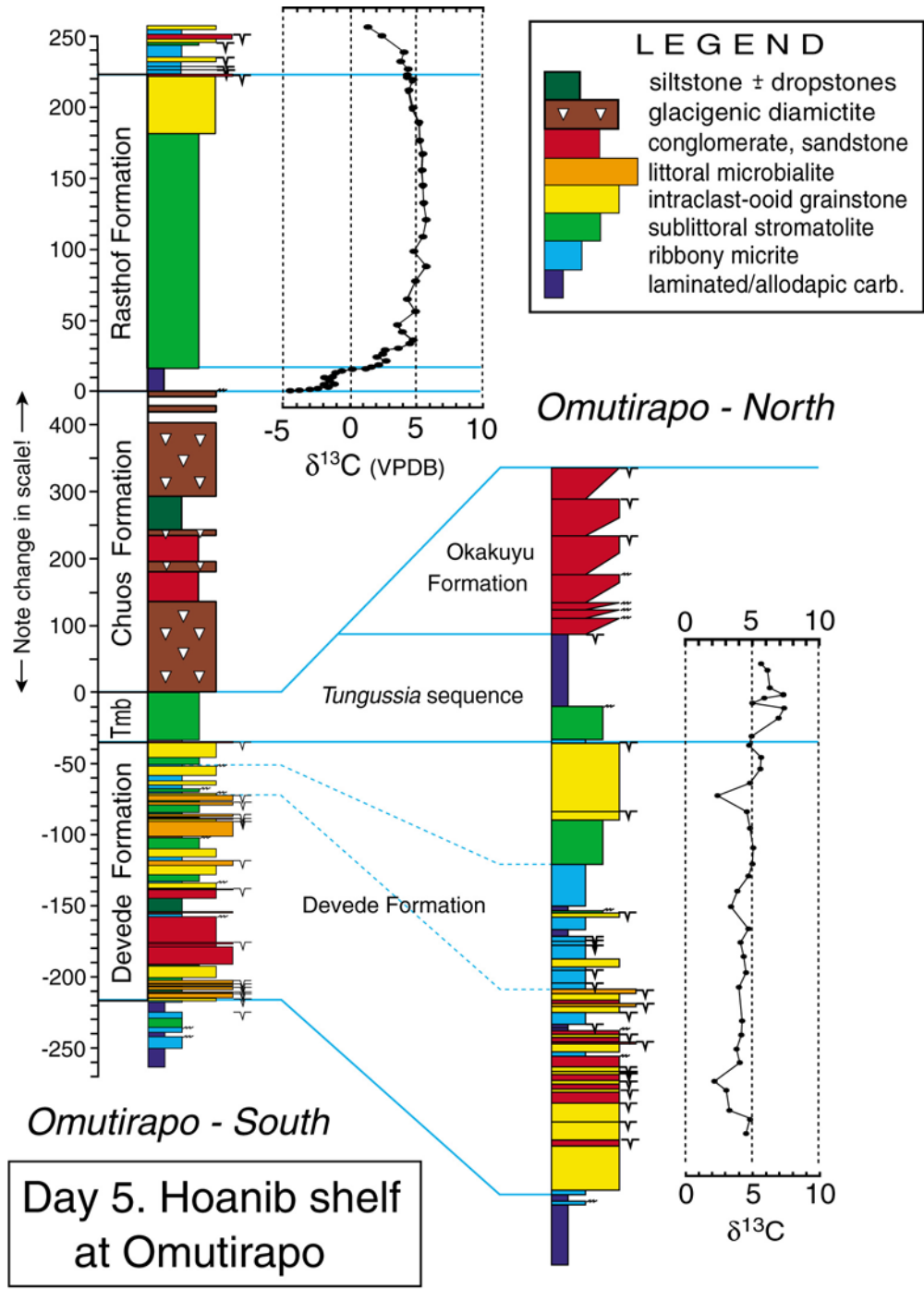


Fig. 14. Columnar sections and carbon isotopic data for Day 5.

[5-5] **Chuoss-Rasthof contact.** Black dolomitic limestone of the lower Rasthof caps the ridge and the contact with diamictite is well exposed at the south “nose” of the ridge. The top of the diamictite is characteristically haematite-rich. The base of the cap carbonate, discoloured by haematite, is a smooth sharp contact, with no evidence of reworking or subaerial exposure. The basal 12 m of the Rasthof is abiotically laminated on a mm-scale, with a few cm-scale allodapic layers that increase in abundance to the south. The top of the laminated unit is an abrupt transition, observed regionally, to convoluted microbialaminite that continues upward for >100 m. Unless you are very fond of severe macrokarst hosting untouched grass for good reason, you are advised to descend into the small river bed draining from the north, along which the outcrops of microbialaminite are more decipherable.

[5-6] **Lower Rasthof sublittoral microbialaminite.** The Rasthof microbialaminite is not a littoral zone deposit. It continues for >100 m vertical without evidence of subaerial exposure or absence of microbial activity. It extends over >10⁴ km² and appears to be a “deep” sublittoral shelf deposit. The microbial lamination is ubiquitously convoluted and intense karstification makes it difficult to study or photograph. The sand-blasted outcrops on the river course are unusually instructive. The convolute structures have previously been attributed to slumping, and as a part-time structural geologist I am struck by the association of antiformal structures with ramp-like dislocation surfaces. But if they are analogous to thrust anticlines, there appears to be no preferred azimuth of vergence. Lateral microbial growth expansion might theoretically produce such convolutions in cohesive, pliable, well-laminated sediment. Of course, such a condition would favour slumping on any seismically active paleoslope. There is some evidence here for phototrophism (e.g., coniform caps on growing antiforms), suggesting that the microbial mats were at least at times within the photic zone.

This ends the short-day traverse to the south end of the Omutirapo amphitheatre. The IAS Excursion should gather and return together to the vehicles, departing the Rasthof not later than 1420 hrs. The abbreviated notes for sites [5-7] through [5-11] pertain to the optional full-day traverse to the north end of the amphitheatre. Section [5-12] in the middle Rasthof, will be the “dessert” stop for the IAS Excursion.

[5-7] **Middle Ombombo mixed parasequences.** This section is thicker (440 m), more complete and better exposed than the section at [5-2]. The clastics are more distal. Don’t miss the 8-m thick *Conophyton* bed 80 m above the base of the section.

[5-8] **Upper Ombombo stromatolite member.** The *Tungussia* stromatolite member is here overlain by ~60 m of marly allodapic limestone. Where exposed, the contact with the overlying fine-grained clastics is erosional.

[5-9] **Upper Ombombo conglomerate.** The retrogradational stack of coarsening-upward clastic cycles culminates, near the top of the section, with a conglomerate containing numerous amygdaloidal basalt pebbles. The volcanism could be related to the Naauwpoort volcanics in the Outjo basin. Their age of 746±2 Ga is compatible with the age of 758±4 Ma for an ash in the upper part of the middle Ombombo subgroup (Hoffman et al., 1996; and unpublished data).

[5-10] **Chuoss diamictite and basal Rasthof Formation.** The Chuoss diamictite is only 20 m thick, compared with 450 m at [5-4] and the Rasthof cap-carbonate sequence is also unusually condensed related to movement on the f1 fault. The Chuoss-Rasthof contact is exposed near the southern “nose” of the Rasthof-capped ridge. Looking south, you can trace the charcoal-grey Rasthof in the distant hills, and see the gently-curved, glacial-cut, side walls of the main valley. The view from the abandoned dwellings near the top of the travertine platform is marvellous.

[5-11] **Chuosi diamictite.** A clean exposure of Chuosi diamictite occurs at a dry waterfall on the west margin of the travertine platform. To return to camp, follow the trail southward contouring in the Chuosi. The exact indicated route (Fig. 11) affords a comfortable descent through the precipitous conglomeratic sandstones of the upper Ombombo. The walk back takes at least an hour in daylight.

[5-12] **Middle Rasthof microbial roll-ups.** The IAS Excursion will exit the amphitheatre and return south on the main track for **18.5 km** to the base of the section at [5-12], which begins ~55 m above the base of the Rasthof (Fig. 15). The microbialaminite is less convoluted at this level. There are numerous examples of “roll-up” structures, loose strips of microbial mat that have become rolled like French *crêpes*. They indicate that the mats were cohesive but pliable on the sea floor. Not far up-section, there are discordant zones of syn-sedimentary breccia, possibly related to fluid or gas escape.

The section ascending from [5-12] is one of the most accessible continuous sections from Rasthof to lower Elandshoek (Fig. 15). The full 400 m climb takes the better part of a day, but is well worth it if you have the time. Follow the indicated route—the black limestone cliffs of the lower Ombaatjie Formation are technical in most other places. The Ghaub diamictite and Keilberg cap dolostone are better developed near *Khowarib Schlucht*, and the IAS Excursion will proceed there. Drive south for **5.7 km** to Ombaatjie (Fig. 17), then turn right and find the track heading west that enters the range along the north bank of the Hoanib River. Follow this track for **6.2 km** (11.9 km), then pull off to right and descend toward the large side-valley draining from the northeast. We will camp on the flats near the mouth of the side-valley.

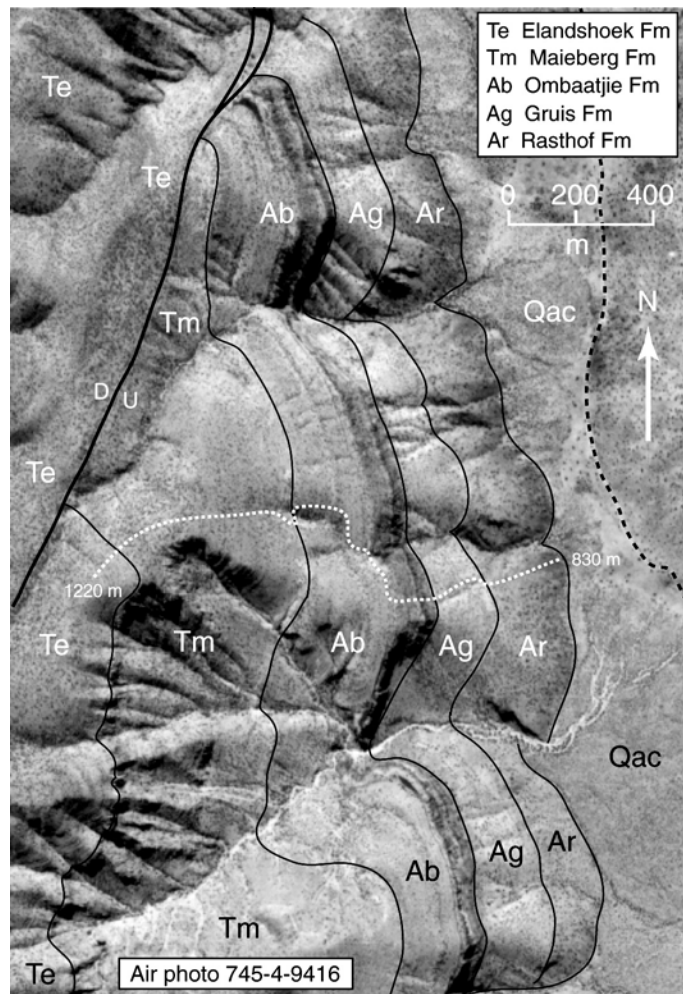


Fig. 15. Photo map for Stop 5-12. Day trip to the top offers accessible section from middle Rasthof to lower Elandshoek. Excursion will examine the Rasthof only. Geology by P.F. Hoffman.

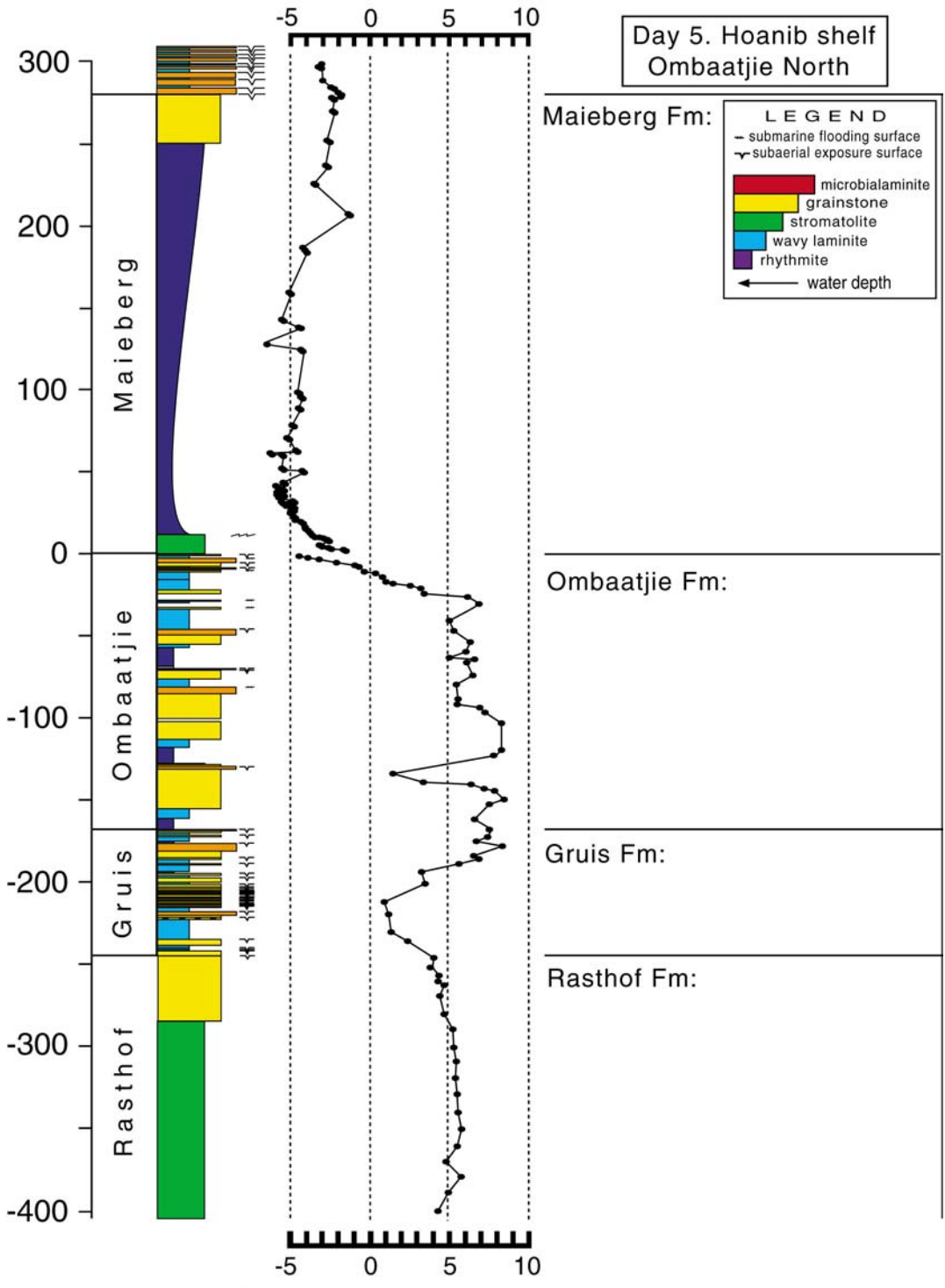


Fig. 16. Columnar section and carbon isotopic data for Stop 5-12.

Day 6. Ghaub glaciation on the Hoanib shelf

(Lat. 19° 18.8'S, long. 13° 59.25'E near Khowarib Schlucht)

We previously examined carbonates bounding the Ghaub glaciation on the margin (Day 2) and foreslope (Day 3) of the platform. We end the excursion with a section of the same interval on the Hoanib shelf (Fig. 3). We will traverse on foot for ca 1.2 km up the side valley and then ascend to the right (Fig. 17). The pale dolostone unit making the first ledge is the Keilberg cap dolostone. Use binoculars to pick the one shallow drainage that offers a continuous clean bedrock section through the recessive interval directly above the Keilberg. This same section offers expansive clean exposure of the Keilberg stromatolites and their tubular structures, as well as Ghaub diamictite and the uppermost Ombaatjie platform. The columnar section [6-1] with isotopic data is given in Fig. 19. We will have until 1220 hrs to examine the section, at which time we must return to the vehicles and make the ca 6.5 hr drive to Outjo and the Hotel Onduri.

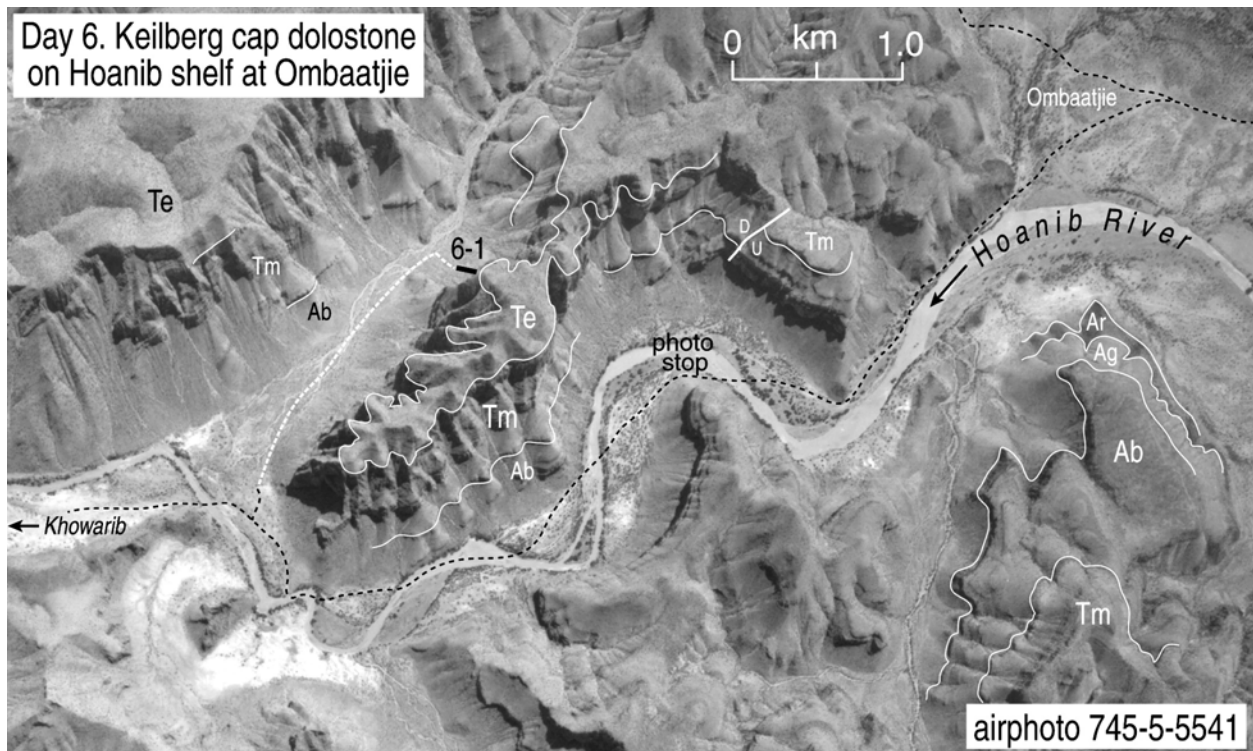


Fig. 17. Photo map for Day 6. Stop 6-1 is on the back side of the cliff shown in Fig. 18. Geology by P.F. Hoffman.

[6-1] **Keilberg cap dolostone and associated strata on the Hoanib shelf.** The section exposes 10 m of uppermost Ombaatjie dolostone, probably belonging to parasequence 7. Coarsening-upward grainstone is capped by a 2.4 m stromatolite, possibly correlative with the stromatolite on the Huab dip-slope at Tweelingskop [2-3]. The Ghaub carbonate diamictite has abrupt lower and upper contacts and ranges in thickness from 10 cm in the main section to 1.5 m on the next ridge ca 100 m to the northeast. The basal metre of the Keilberg is hummocky cross-laminated and lacks tubular structures. The latter are strictly confined within stromatolites, which develop at nodes, expand upwards, and coalesce laterally. The relation between the faint but strongly arched stromatolitic laminae and the meniscus-type lamination within the tubular structures is much better preserved than at the margin of the platform. The stromatolitic interval is 3.2 m thick and highly continuous laterally. Return to the main line of section and climb to the upper Keilberg member at the dry waterfall. Above the stromatolite, hummocky cross-lamination returns and there are typical examples of the enigmatic “pseudo-tepee” structures. Their axes strike 120° and axial planes dip to the southwest. The top of the Keilberg member is a flooding surface 18.5 m above the base, above which are 60 m of rhythmically alternating greenish-pink limestone and impure, tan-coloured, allodapic dolostone. A green calc-silicate mineral (tremolite?) appears in this interval. The gully gives easy access to an additional 200

m of pink and grey allodapic limestone with abundant hummocky cross-stratification. $^{87}\text{Sr}/^{86}\text{Sr}$ ratios in these limestones are uniformly 0.7075 (unpublished data). The upper part of the Maieberg cap-carbonate sequence cannot be reached in this section without wings (see Fig. 18).

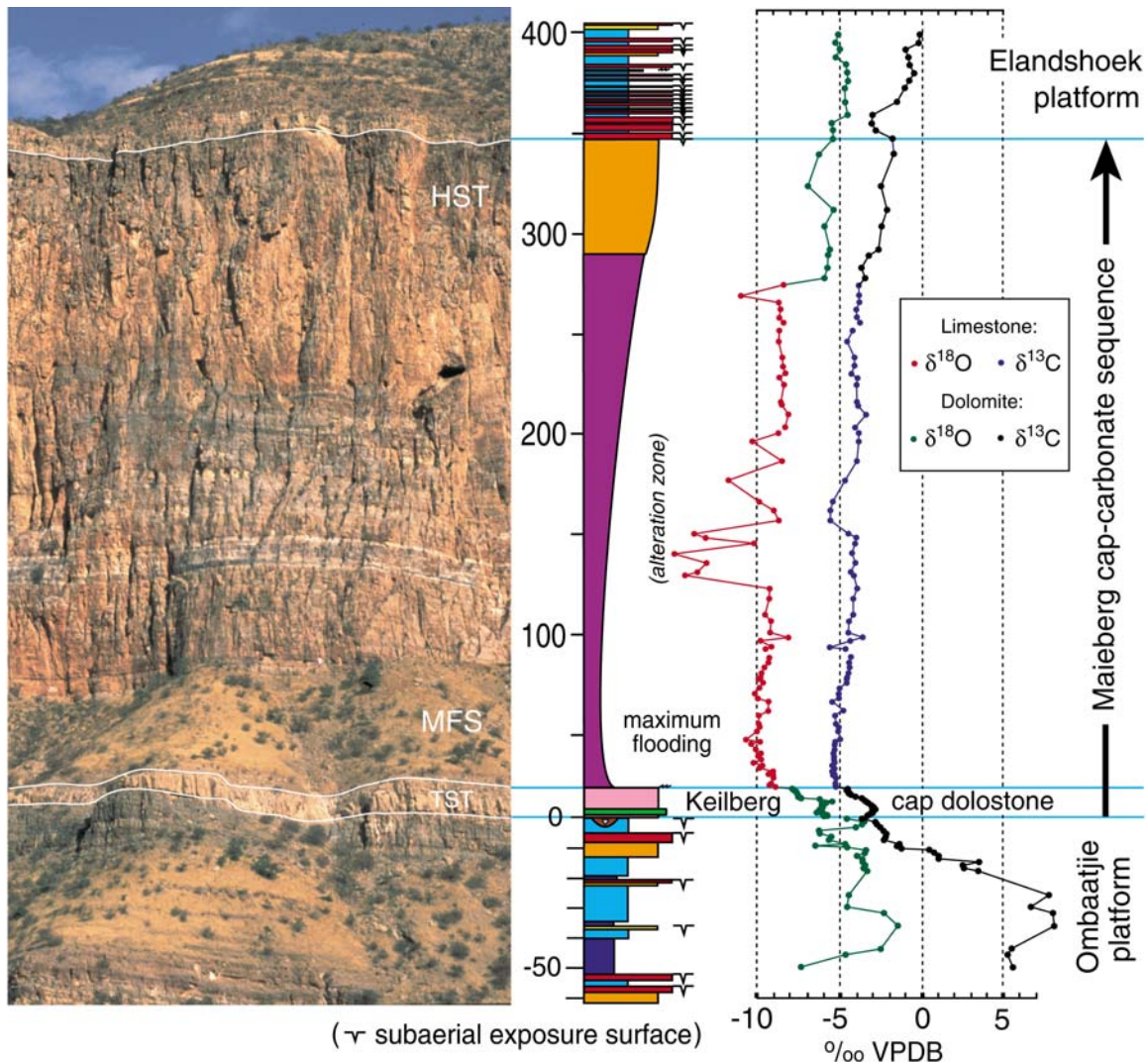


Fig. 18. Carbon and oxygen isotopic data for Day 6. Upper Ombaatjie data is from the section shown in the photo. Maieberg data is from Stop 6-1, on the back side of the ridge. Note change in vertical section at the datum, necessitated by the perspective effect.

Day 6. Ghaub glaciation on Hoanib shelf at Stop 6-1.

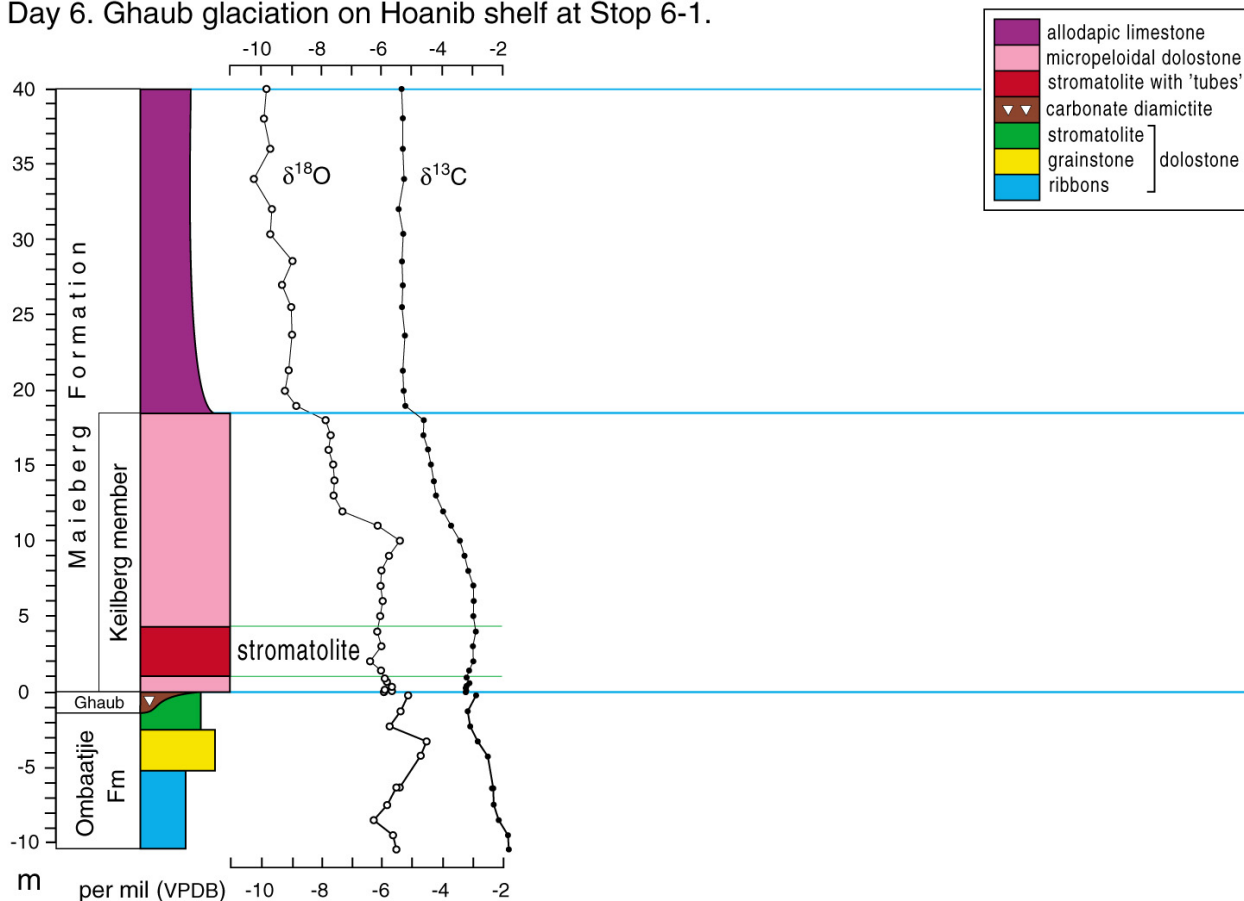


Fig. 19. Columnar section with carbon and oxygen isotopic data for Stop 6-1. The isotopic profiles are closely similar to a correlative section in the Otavi Mountains 350 km to east.

To reach Outjo, backtrack 6.2 km along the Hoanib River to *Ombaatjie* (6.2 km). Then head south-southeast, reversing the route taken on Day 4, reaching the main gravel road (C35) with the daily odometer reading 49.7 km. Turn right and continue southeast on **C35** to *Kamanjab* (103.6 km). Refuel at the Shell station. Then take the sealed road (**C40**) heading east for 146 km to the junction with C38 (250 km). Turn right onto **C38** and head south for 9 km to *Outjo* (259 km). The Hotel Onduri is on the right, just before the town square.

Day 7. Outjo to Windhoek

Retrace the route taken in Day 1, C38 to Otjiwarongo, then B1 south via Okahandja, arriving in Windhoek around 1230 hrs.

ACKNOWLEDGEMENTS

The work behind this guidebook was funded by the Tectonics and Earth Systems History programs of the United States National Science Foundation and the NASA Astrobiology Institute. Additional support came from the Geological Survey of Namibia, the Canadian Institute for Advanced Research, and Harvard University. I gratefully acknowledge the enthusiastic assistance of many students during this work and the observations of participants on previous field excursions. I am particularly indebted to Galen P. Halverson for field work over five seasons and for most of the isotopic measurements.

REFERENCES CITED

- Babinski, M., Chemale, Jr., F., Hartmann, L.A., Van Schmus, W.R. and da Silva, L.C.** (1996) Juvenile accretion at 750-700 Ma in southern Brazil. *Geology*, **24**, 439-442.
- Babinski, M., Chemale, Jr., F., Van Schmus, W.R., Hartmann, L.A. and da Silva, L.C.** (1997) U-Pb and Sm-Nd geochronology of the Neoproterozoic granitic-gneissic Dom Feliciano belt, southern Brazil. *J. South Afr. Earth Sci.*, **10**, 263-274.
- Brasier, M., McCarron, G., Tucker, R., Leather, J., Allen, P. and Shields, G.** (2000) New U-Pb zircon dates for the Neoproterozoic Ghubrah glaciation and for the top of the Huqf Supergroup, Oman. *Geology*, **28**, 175-178.
- Cahen, L. and Lepage, J.** (1981) Proterozoic diamictites of Lower Zaire. In: *Earth's Pre-Pleistocene Glacial Record* (Ed. M.J. Hambrey and W.B. Harland), pp. 162-166. Cambridge University Press, Cambridge.
- Caldeira, K. and Kasting, J.F.** (1992) Susceptibility of the early Earth to irreversible glaciation caused by carbon dioxide clouds. *Nature*, **359**, 226-228.
- Canfield, D.E. and Raiswell, R.** (1999) The evolution of the sulfur cycle. *Am. J. Sci.*, **299**, 697-723.
- Cloud, P.E., Wright, L.A., Williams, E.G., Diehl, P., and Walter, M.R.** (1974) Giant stromatolites and associated vertical tubes from the Upper Proterozoic Noonday Dolomite, Death Valley region, eastern California. *Geol. Soc. Am. Bull.*, **85**, 1869-1882.
- Crawford, A.R. and Daily, B.** (1971) Probable non-synchronicity of Late Precambrian glaciations. *Nature*, **230**, 111-112.
- Condon, D.L., Prave, A.R., and Benn, D.I.** (2002) Neoproterozoic glacial-rainout intervals: observations and implications. *Geology*, **30**, p. 35-38.
- Coward, M.P.** (1981) The junction between Pan-African mobile belts in Namibia: its structural history. *Tectonophysics*, **76**, 59-73.
- Crowell, J.C.** (1983) Ice ages recorded on Gondwanan continents, Du Toit Memorial Lecture No. 18. *Geol. Soc. S. Afr. Trans.*, **86**, 237-262.
- Embleton, B.J.J. and Williams, G.E.** (1986) Low palaeolatitude of deposition for late Precambrian periglacial varvites in South Australia: implications for paleoclimatology. *Earth Planet. Sci. Lett.*, **79**, 419-430.
- Emanuel, K.A.** (1999) Thermodynamic control of hurricane intensity. *Nature*, **401**, 665-669.
- Evans, D.A.D.** (2000) Stratigraphic, geochronological, and paleomagnetic constraints upon the Neoproterozoic climatic paradox. *Am. J. Sci.*, **300**, 347-433.
- Daly, M.C., Lawrence, S.R., Diemu-Tshiband and Matouana, B.** (1992) Tectonic evolution of the Cuvette Centrale, Zaire. *J. Geol. Soc., Lond.*, **149**, 539-546.
- Dunn, P.R., Thomson, B.P., and Rankama, K.** (1971) Late Precambrian glaciation in Australia as a stratigraphic boundary. *Nature*, **231**, 498-502.
- Eyles, N.** (1993) Earth's glacial record and its tectonic setting. *Earth-Science Rev.*, **35**, 1-248.
- Fairchild, I.J.** (1993) Balmy shores and icy wastes: the paradox of carbonates associated with glacial deposits in Neoproterozoic times. In: *Sedimentology Review 1* (V.P. Wright, ed.), pp. 1-16, Blackwell Scientific Publications, Oxford.
- Fölling, P.G. and Frimmel, H.E.** (2002) Chemostratigraphic correlation of carbonate successions in the Gariep and Saldania belts, Namibia and South Africa. *Basin Research*, **14**, 69-88.
- Frets, D.C.** (1969) Geology and structure of the Huab-Welwitschia area, South West Africa. *Bull. Precamb. Res. Unit, Univ. Cape Town*, **5**, 235 pp.
- Frimmel, H.E., Klötzli, U.S. and Siegfried, P.R.** (1996) New Pb-Pb single zircon age constraints on the timing of Neoproterozoic glaciation and continental break-up in Namibia. *J. Geol.*, **104**, 459-469.
- Geological Survey of Namibia** (undated) *Aeromagnetic Anomaly Map of Namibia*. Geological Survey of Namibia, Windhoek.
- Germs, G.J.B.** (1995) The Neoproterozoic of southwestern Africa, with emphasis on platform stratigraphy and paleontology. *Precambrian Res.*, **73**, 137-151.
- Grant, S.W.F.** (1990) Shell structure and distribution of Cloudina, a potential index fossil for the terminal Proterozoic. *Am. J. Sci.*, **290-A**, 261-294.
- Grotzinger, J.P. and James, N.P.** (2000) Precambrian carbonates: evolution of understanding. In: *Carbonate Sedimentation and Diagenesis in the Evolving Precambrian World* (J.P. Grotzinger and N.P. James, eds.), SEPM (Society for Sedimentary Geology) Spec. Pub., **67**, 3-20.

- Grotzinger, J.P. and Knoll, A.H.** (1995) Anomalous carbonate precipitates: Is the Precambrian the key to the Permian? *Palaios*, **10**, 578-596.
- Grotzinger, J.P., Watters, W.A. and Knoll, A.H.** (2000) Calcified metazoans in thrombolite-stromatolite reefs of the terminal Proterozoic Nama Group, Namibia. *Paleobiology*, **26**, 334-359.
- Grotzinger, J.P., Bowring, S.A., Saylor, B.Z. and Kaufman, A.J.** (1995) Biostratigraphy and geochronologic constraints on early animal evolution. *Science*, **270**, 598-604.
- Guj, P.** (1970) The Damara mobile belt in the south-western Kaokoveld, South West Africa. *Bull. Precamb. Res. Unit, Univ. Cape Town*, **8**, 168 pp.
- Halverson, G.P., Hoffman, P.F., Schrag, D.P., and Kaufman, A.J.** (2002) A major perturbation of the carbon cycle before the Ghaub glaciation (Neoproterozoic) in Namibia: a trigger mechanism for snowball Earth. *Geochem. Geophys. Geosystems*, in press.
- Hambrey, M.J. and Harland, W.B.** (1981) *Earth's Pre-Pleistocene Glacial Record*. Cambridge University Press, Cambridge, 1004 pp.
- Harland, W.B.** (1964) Evidence of Late Precambrian glaciation and its significance. In: *Problems in Palaeoclimatology* (A.E.M. Nairn, ed.), pp. 119-149, 180-184, Interscience, John Wiley & Sons, London.
- Hedberg, R.M.** (1979) Stratigraphy of the Ovamboland Basin, South West Africa. *Bull. Precamb. Res. Unit, Univ. Cape Town*, **24**, 325 pp.
- Hegenberger, W.** (1987) Gas escape structures in Precambrian peritidal carbonate rocks. *Communs. Geol. Surv. S.W. Africa/Namibia*, **3**, 49-55.
- Hegenberger, W.** (1993) Stratigraphy and sedimentology of the Late Precambrian Witvlei and Nama Groups, east of Windhoek. *Geol. Surv. Namibia Mem.*, **17**, 82 pp.
- Henry, G., Clendenin, C.W., Stanistreet, I.G. and Maiden, K.J.** (1990) Multiple detachment model for the early rifting stage of the Late Proterozoic Damara orogen. *Geology*, **18**, 67-71.
- Higgins, J.** (2002) *The Aftermath of a Snowball Earth*. B.A. thesis, Harvard College, Cambridge, MA, USA.
- Hoffman, P.F. and Hartz, E.H.** (1999) Large, coherent, submarine landslide associated with Pan-African foreland flexure. *Geology*, **27**, 687-690.
- Hoffman, P.F. and Schrag, D.P.** (2000) Snowball Earth. *Sci. Am.*, **282**, 62-75.
- Hoffman, P.F. and Schrag, D.P.** (2002) The snowball Earth hypothesis: testing the limits of global change. *Terra Nova*, **14**, 000-000.
- Hoffman, P.F., Halverson, G.P., and Grotzinger, J.P.** (2002) Are Proterozoic cap carbonates and isotopic excursions a record of gas hydrate destabilization following Earth's coldest intervals? *Comment. Geology*, **30**, 286-287.
- Hoffman, P.F., Hawkins, D.P., Isachsen, C.E. and Bowring, S.A.** (1996) Precise U-Pb zircon ages for early Damaran magmatism in the Summas Mountains and Welwitschia inlier, northern Damara belt, Namibia. *Communs. Geol. Surv. Namibia*, **11**, 47-52.
- Hoffman, P.F., Kaufman, A.J., Halverson, G.P., and Schrag, D.P.** (1998) A Neoproterozoic snowball Earth. *Science*, **281**, 1342-1346.
- Hoffmann, K.H.** (1987) Application of tectonostratigraphic terrane analysis in the Damara Province of central and northern Namibia. In: *Abstract Volume. A.L. du Toit Golden Jubilee Conference on Tectonostratigraphic Terrane Analysis*, pp. 25-27. Royal Society and Geological Society South Africa, Cape Town.
- Hoffmann, K.-H. and Prave, A.R.** (1996) A preliminary note on a revised subdivision and regional correlation of the Otavi Group based on glaciogenic diamictites and associated cap dolostones. *Communs. Geol. Surv. Namibia*, **11**, 77-82.
- Hyde, W.T., Crowley, T.J., Baum, S.K., and Peltier, W.R.** (2000) Neoproterozoic 'snowball Earth' simulations with a coupled climate/ice-sheet model. *Nature*, **405**, 425-429.
- Jacobsen, S.B. and Kaufman, A.J.** (1999) The Sr, C and O isotopic evolution of Neoproterozoic seawater. *Chem. Geol.*, **161**, 37-57.
- James, N.P., Narbonne, G.M., and Kyser, T.K.** (2001) Late Neoproterozoic cap carbonates: Mackenzie Mountains, northwestern Canada: precipitation and global glacial meltdown. *Can. J. Earth Sci.*, **38**, 1229-1262.
- Kaufman, A.J., Knoll, A.H., and Narbonne, G.M.** (1997) Isotopes, ice ages, and terminal Proterozoic earth history. *Proc. Natl. Acad. Sci. USA*, **94**, 6600-6605.
- Kaufman, A.J., Hayes, J.M., Knoll, A.H., and Germs, G.J.B.** (1991) Isotopic compositions of carbonates and organic carbon from upper Proterozoic successions in Namibia: stratigraphic variation and the effects of diagenesis and metamorphism. *Precambrian Res.*, **49**, 301-327.

- Kauffman, E.G., Arthur, M.A., Howe, B., and Scholle, P.A.** (1996) Widespread venting of methane-rich fluids in Late Cretaceous (Campanian) submarine springs (Tepee Buttes), Western Interior seaway, U.S.A. *Geology*, **24**, 799-802.
- Kendall, C.G.St.C. and Warren, J.** (1987) A review of the origin and setting of tepees and their associated fabrics. *Sedimentology*, **34**, 1007-1028.
- Kennedy, M.J.** (1996) Stratigraphy, sedimentology, and isotope geochemistry of Australian Neoproterozoic postglacial cap dolostones: deglaciation, $\delta^{13}\text{C}$ excursions, and carbonate precipitation. *J. Sed. Res.*, **66**, 1050-1064.
- Kennedy, M.J., Christie-Blick, N., and Prave, A.R.** (2001a) Carbon isotopic composition of Neoproterozoic glacial carbonates as a test of paleoceanographic models for snowball Earth phenomena. *Geology*, **29**, 1135-1138.
- Kennedy, M.J., Christie-Blick, N., and Sohl, L.E.** (2001b) Are Proterozoic cap carbonates and isotopic excursions a record of gas hydrate destabilization following Earth's coldest intervals. *Geology*, **29**, 443-446.
- Kennedy, M.J., Runnegar, B., Prave, A.R., Hoffmann, K.-H., and Arthur, M.A.** (1998) Two or four Neoproterozoic glaciations? *Geology*, **26**, 1059-1063.
- King, C.H.M.** (1994) *Carbonates and mineral deposits of the Otavi Mountainland*. Proterozoic Crustal & Metallogenic Evolution, Excursion 4, 40 pp. Geological Society and Geological Survey of Namibia, Windhoek.
- Kirschvink, J.L.** (1992) Late Proterozoic low-latitude global glaciation: the snowball earth. In: *The Proterozoic Biosphere* (J.W. Schopf and C. Klein, eds.), pp. 51-52, Cambridge University Press, Cambridge.
- Klein, C. and Beukes, N.J.** (1993) Sedimentology and geochemistry of the glaciogenic late Proterozoic Rapitan iron-formation in Canada. *Econ. Geol.*, **84**, 1733-1774.
- Kröner, A.** (1977) Non-synchronicity of Late Precambrian glaciations in Africa. *J. Geol.*, **85**, 289-300.
- Kukla, P.A. and Stanistreet, I.G.** (1991) Record of the Damara Khomas Hochland accretionary prism in central Namibia: refutation of an "ensialic" origin of a Late Proterozoic orogenic belt. *Geology*, **19**, 473-476.
- Martin, H.** (1965) *The Precambrian geology of South West Africa and Namaqualand*. Precambrian Research Unit, University of Cape Town, South Africa, 159 pp.
- Martin, H., Porada, H. and Walliser, O.H.** (1985) Mixtite deposits of the Damara sequence, Namibia, problems of interpretation. *Palaeogeogr. Palaeoclimat. Palaeoecol.*, **51**, 159-196.
- Mawson, D.** (1949a) The late Precambrian ice-age and glacial record of the Bibliando dome. *J. and Proc. Roy. Soc. New South Wales*, **82**, 150-174.
- McElhinny, M.W., Giddings, J.W., and Embleton, B.J.J.** (1974) Palaeomagnetic results and late Precambrian glaciations. *Nature*, **248**, 557-561.
- McMechan, M.E.** (2000a) Vreeland diamictites—Neoproterozoic glaciogenic slope deposits, Rocky Mountains, northeast British Columbia. *Can. Bull. Petrol. Geol.*, **48**, 246-261.
- McMechan, M.E.** (2000b) Reply to discussion. Vreeland diamictites—Neoproterozoic glaciogenic slope deposits, Rocky Mountains, northeast British Columbia. *Can. Bull. Petrol. Geol.*, **48**, 364-366.
- Meert, J. G., Van der Voo, R. and Ayub, S.** (1995) Paleomagnetic investigation of the Neoproterozoic Gagwe lavas and Mbozi complex, Tanzania and the assembly of Gondwana. *Precambrian Res.* **74**, 225-244.
- Miller, R.McG.** (1980) Geology of a portion of central Damaraland, South West Africa/Namibia. *Publ. geol. Surv. Namibia*, **6**, 1-78.
- Miller, R.McG.** (1983) The Pan-African Damara orogen of South West Africa/ Namibia. In: *Evolution of the Damara Orogen* (Ed. R.McG. Miller), *Spec. Publ. geol. Soc. S. Afr.*, **11**, 431-515.
- Miller, R.McG.** (1997) The Owambo basin of northern Namibia. In: *African Basins. Sedimentary Basins of the World*, 3 (Ed. R.C. Selley), pp. 237-268. Elsevier, Amsterdam.
- Porada, H., Ahrendt, H., Behr, H.-J. and Weber, K.** (1983) The join of the coastal and intracontinental branches of the Damara orogen, Namibia, In: *Intracontinental fold belts* (edited by Martin, H. and Eder, F. W.). Springer-Verlag, Berlin, 901-912.
- Preiss, W.V.** (2000) The Adelaide geosyncline of South Australia and its significance in Neoproterozoic continental reconstruction. *Precambrian Res.*, **100**, 21-63.
- Runnegar, B.** (2000) Loophole for snowball Earth. *Nature*, **405**, 403-404.
- SACS (South African Committee for Stratigraphy)** (1980) Damara sequence. In: Kent, L.E., Comp. Stratigraphy of South Africa, Part 1. *Handbook Geol. Surv. S. Afr.*, **8**, 415-438.
- Saylor, B.Z., Kaufman, A.J., Grotzinger, J.P. and Urban, F.** (1998) A composite reference section for terminal Proterozoic strata of southern Namibia. *J. Sed. Res.*, **68**, 1223-1235.

- Schermerhorn, L.J.G. and Stanton, W.I.** (1963) Tilloids in the West Congo geosyncline. *Quart. J. Geol. Soc. Lond.*, **119**, 201-241.
- Schrag, D.P., Berner, R.A., and Hoffman, P.F.** (2002) On the initiation of a snowball Earth. *Geochem. Geophys. Geosystems*, in press.
- Shields, G., Stille, P., Brasier, M.D. and Atudorei, N.-V.** (1997) Stratified oceans and oxygenation of the late Precambrian environment: a post glacial geochemical record from the Neoproterozoic of W. Mongolia. *Terra Nova*, **9**, 218-222.
- Schmidt, P.W. and Williams, G.E.** (1995) The Neoproterozoic climatic paradox: equatorial paleolatitude for Marinoan glaciation near sea level in South Australia. *Earth Planet. Sci. Lett.*, **134**, 107-124.
- Schmidt, P.W., Williams, G.E., and Embleton, B.J.J.** (1991). Low palaeolatitude of Late Proterozoic glaciation: early timing of remanence in haematite of the Elatina Formation, South Australia. *Earth Planet. Sci. Lett.*, **105**, 355-367.
- Soffer, G.** (1998). *Evolution of a Neoproterozoic continental margin subject to tropical glaciation*. B.A. thesis, Harvard College, Cambridge, MA.
- Sohl, L.E., Christie-Blick, N., and Kent, D.V.** (1999) Paleomagnetic polarity reversals in Marinoan (ca. 600 Ma) glacial deposits of Australia: implications for the duration of low-latitude glaciations in Neoproterozoic time. *Geol. Soc. Am. Bull.*, **111**, 1120-1139.
- Spencer, A.M.** (1971) Late Pre-Cambrian glaciation in Scotland. *Mem. Geol. Soc. Lond.*, **6**, 11 pp.
- Stanistreet, I.G., Kukla, P.A., and Henry, G.** (1991) Sedimentary basinal response to a Late Precambrian Wilson cycle: the Damara orogen and Nama foreland, Namibia. *J. Afr. Earth Sci.*, **13**, 141-156.
- Walter, M.R., Veevers, J.J., Calver, C.R., Gorjan, P., and Hill, A.C.** (2000) Dating the 840-544 Ma Neoproterozoic interval by isotopes of strontium, carbon, and sulfur in seawater, and some interpretive models. *Precambrian Res.*, **100**, 371-433.
- Warren, S.G., Brandt, R.E., Grenfell, T.C., and McKay, C.P.** (2002) Snowball Earth: ice thickness on the tropical ocean. *J. Geophys. Res. (Oceans)*, in press.
- Wright, L., Williams, E.G., and Cloud, P.** (1978) Algal and cryptalgal structures and platform environments of the late pre-Phanerozoic Noonday Dolomite, eastern California. *Geol. Soc. Am. Bull.*, **89**, 321-333.